OVERCOMING CHALLENGES FOR SKIN DEPOSITION OF DRUGS: SiRNA AND ANTIMICROBIAL AGENTS

BY

MANIA DORRANI

A Dissertation submitted to the

Graduate School-New Brunswick

Rutgers, the State University of New Jersey

In partial fulfillment of the requirements

For the degree of

Doctor of Philosophy

Graduate Program in Pharmaceutical Sciences

Written under the direction of

Professor Bozena Michniak-Kohn, Ph.D.

And approved by

_____

_____

_____

_____

_____

New Brunswick, New Jersey

May, 2017

ABSTRACT OF THE DISSERTATION
OVERCOMING CHALLENGES FOR SKIN DEPOSITION OF DRUGS: SiRNA AND ANTIMICROBIAL AGENTS

BY MANIA DORRANI

Dissertation Director:

Bozena Michniak-Kohn, Ph.D.

Delivery of macromolecules such as siRNA into cells that reside in the basal epidermis of the skin is a major challenge due to the transport barriers that need to be overcome. siRNAs have potential therapeutic applications in various dermatological diseases such as psoriasis, atopic dermatitis, and cancer. Unfortunately, thelow permeability of siRNA through the stratum corneum and epidermis has significantly limited its use for topical application. There are two important factors that specify permeation and deposition of molecules into the skin. One is the membrane properties, and the second is the molecule properties. The *objective* of this study was to develop a topical siRNA delivery system that can permeate through the stratum corneum and viable epidermis and efficiently deposit therapeutic levels of siRNA to the basal epidermis/upper dermis where melanoma cells reside. To achieve this objective, we first compared permeation rate variation of different hydrophilic and lipophilic compounds through the human cadaver skin samples and two synthetic membranes. Afterward, in order to specify molecular properties that can deposit into the skin, we formulated two lipophilic antimicrobial agents and compared their skin deposition and permeation rate. At the end, we formulated series of liposome compositions that contained various concentrations of edge activator in their structures and then complexed with siRNA at

different ratios to generate a small library of liposome-siRNA complexes (lipoplexes) with different physicochemical properties. In this study we used melanoma as a disease model. Through use of quantitative imaging analysis, we identified the necessary design parameters for effective permeation of lipoplexes through the skin layers and deposition at the upper dermis. The ability of the formulated lipoplexes to internalize into melanoma cells, knockdown the expression of the BRAF protein and induce cell death in melanoma cells was studied by fluorescent microscopy, in-cell immunofluorescence assay and WST-1 cell proliferation assay. By providing direct quantitative and qualitative microscopy evidence, the results of this study demonstrate for the first time that the passive delivery of an edge-activated liposomal formulation can effectively carry siRNA through the stratum corneum and deposit it at the lower epidermis/upper dermis.

DEDICATIONS

To my beloved husband, Arash;

Who supported me with his unconditional love during all moments.

To my beautiful daugther, Viana;

Who fills my life with love and happiness.

To my parents, Mahvash and Kourosh;

Who were always there for me so that I achieve my dreams.

To my advisor, Dr. Bozena Michniak-Kohn;

Who taught me to think scientifically and work independently.

To my co-advisor, Dr. Tamara Minko;

Whom I couldn’t finish my PhD without her continuous support.

To my sister, Andia

Who is my best friend forever.

Table of Contents

List of Figures

List of Tables

Chapter 1

Introduction

Skin is the largest organ in our body that as a route for drug delivery has been an interesting option because it provides easy accessibility to targeted cells and provides a non-invasive route for drug administration. In addition, due to the specialized structure of skin, large molecules are prevented from easily penetration into the systemic circulation and hence the systemic toxicity will be minimal [1]. Human skin contains three main layers, epidermis, dermis, and subcutaneous tissue that each layer has highly differentiated cells and has evolved to perform multiple functions such as preventing water loss, eliminating environmental toxins, resisting mechanical stress and contributing in immune responses [2]. The stratum corneum SC, the upper most layer of the epidermis has the principal role in providing this protection to the human body. This layer has a thickness ranging from 10-40μm and consists of 15-20 layers of dead keratinized corneocytes that are embedded in organized lipid bilayers. The role of the SC in protecting the body was first established in 1940s when researches scraped layers of cells with sand paper from abdominal skin in an anesthetized patient and monitored water loss from the skin. They observed that by removing the lowest layers of the SC water flux increased significantly [3, 4]. The water content is less than 13% and this layer is lipophilic in nature. SC has small pore sizes less than 50nm that do not permit molecules larger about 500 g/mol pass passively through the skin [5].

Below the SC is the viable epidermis which is ten times thicker than the SC. The viable epidermis consists of multiple layers of cellular and avascular tissue with a water content of more than 50% and is significantly more hydrophilic compared to the SC. This layer offers less resistance to drug diffusion due to the greater water content in the living

cells [6]. However, the epidermis has intercellular junctions (tight junctions) that prevent diffusion of solutes through the epidermal intercellular pathway and thus provide an additional barrier underneath the SC that controls solutes diffusion and water loss [7]. Furthermore, the viable epidermal cells serve as a negatively charged barrier due to the multilayers of cell membrane phospholipids and hence, hindering internalization of anionic molecules into the viable epidermal cells. The skin layers are shown in **Figure 1.1**.

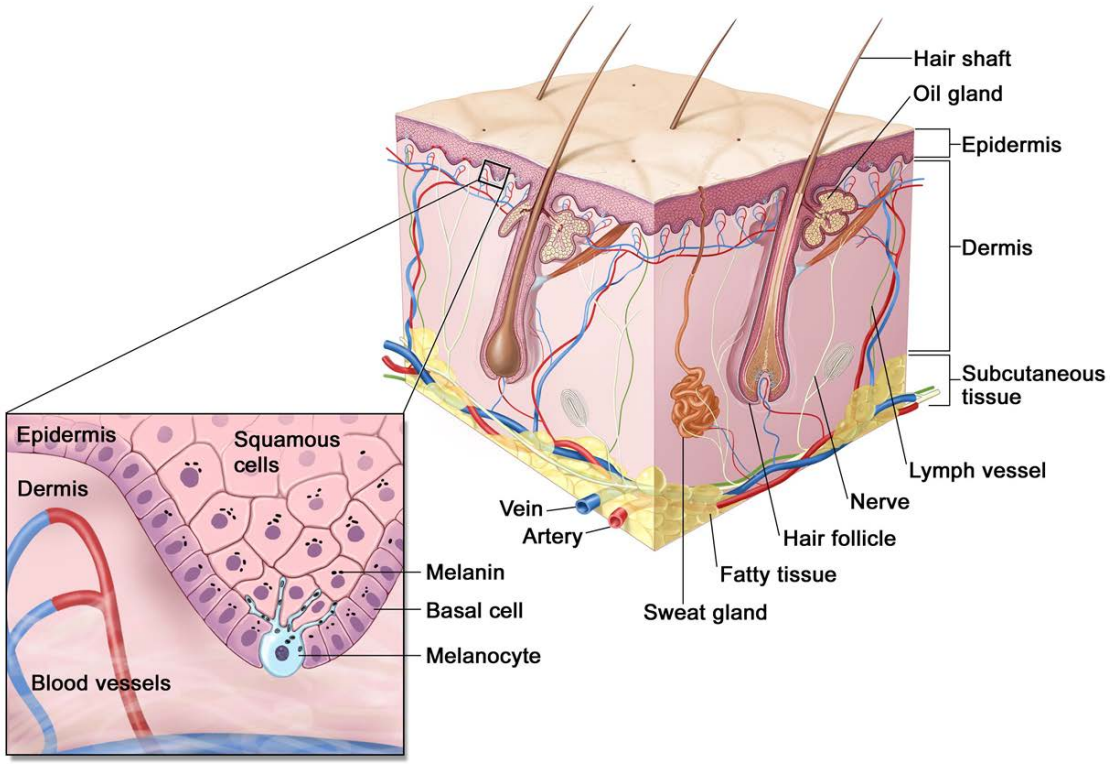

Figure 1.1: Skin layers. The outermost layer of the skin is named stratum corneum (SC) that consists of dead flattened corneocytes. The viable epidermis is a skin layer underneath of the SC and consists of multilayers of keratinocytes and other skin cells. The figure is adapted from national cancer institute.

Three main routes have been identified through SC. 1) Intercellular route: passage of molecules between the corneocytes. 2) Intracellular route: crossing through packed dead cells and the lipid bilayers. 3) Transappendages route: via hair follicles and sweat glands which form bypass pathway through the intact epidermis (**Figure 1.2**). Since the numbers of skin appendages in human skin is less than 0.1%, the third pathway is usually considered of little significance. The intracellular pathway is the most direct route of delivery. However, it requires transport through keratin-filled and lipid-filled corneocytes. The intercellular pathway is thus the more common route for topical drug delivery. In this pathway, the lipid bilayers need to be modified to increase the SC permeability.

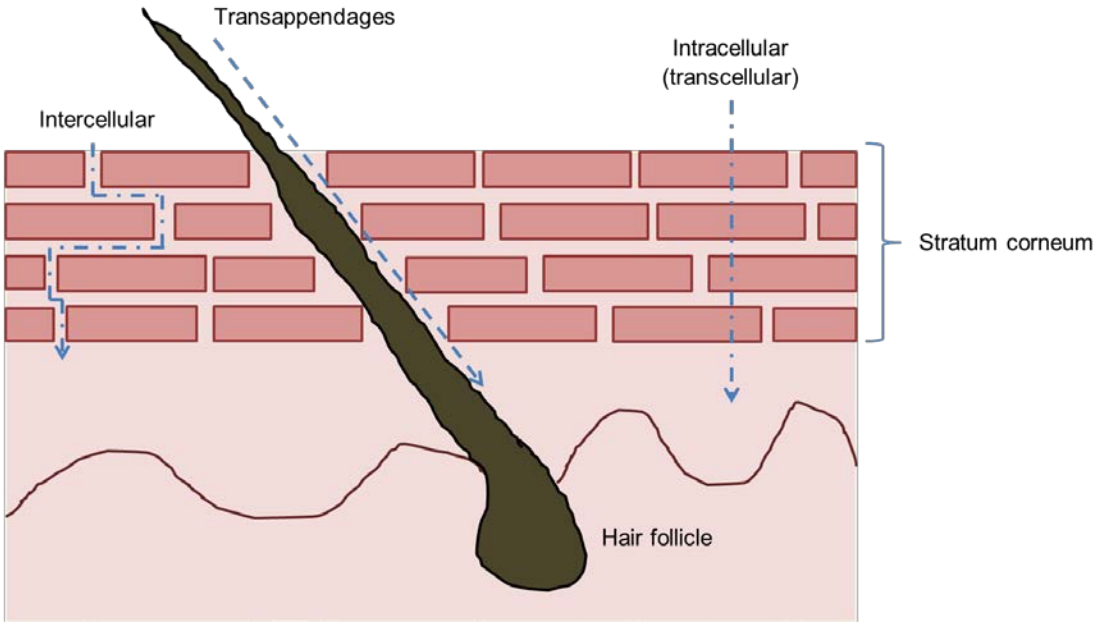

Figure 1.2: Possible pathways of topical drug delivery.

One of the most malignant skin diseases that cause a vast majority of skin cancers death worldwide is melanoma. Based on American Cancer Society report in 2014, on average, one American dies from melanoma every hour and it is estimated that melanoma

incidence rates have been increasing for at least 30 years. Molecular analysis of patients with melanoma shows that approximately 40-60% of melanomas contain a mutation in the gene that encodes BRAF protein. Among BRAF mutations, 90% involves a single point mutation that substitutes Thymine with Adenine at nucleotide 1799. This leads to valine being substituted by glutamic acid at amino acid 600 (V600E) [8]. The BRAF protein is one of the main components of the MAPK cascade (Mitogen-Activated Protein Kinases) in the cell proliferation pathway that transmits extracellular signals to regulate cell functions such as gene expression, apoptosis, cell growth and differentiation [9]. This mutation in the gene encoding BRAF protein activates the downstream signals of the MAP kinase pathway and ultimately causes an oncogenic increase of melanocytes proliferation and division [10]. This mutation originates in the pigment producing skin cells named melanocytes. These cells reside on basal epidermis and normally are responsible for producing melanin in the skin. This gene mutation in melanocytes leads the cells to multiple rapidly and form malignant tumor. If the cancer is not being treated in the first stages of the diagnosis the tumor cells can advance and spread rapidly into other parts of body where it become hard to treat and become fetal. Moreover, screening of 197 patients with BRAF mutated melanoma showed that this type of mutation links with earlier age of onset and shortened survival [11]. The high incidence of mutation in BRAF gene and increased risk of mortality highlight the need of systems that target and inhibit this mutation.

Improvement in molecular analysis of diseases and cancers led to design of more selective and potent technologies. One of these technologies focuses on small interfering RNA (siRNA) mechanism. At late 1990s, Fire et al. synthesized short double stranded

RNA and demonstrated how it can inhibit gene expression at RNA level [12]. In comparison to small molecules, siRNA has a broader therapeutic potential because it provides sequence-specific suppression of any disease associated with gene mutation. Since this Nobel Prize winning discovery, many siRNAs were designed for different gene related diseases. In regard to melanoma, several studies show that BRAF siRNA can selectively pair with the mutated mRNA and silence its expression [13, 14]. (The mechanism of action of siRNA is explained in chapter 2 in details).

For the treatment of skin diseases, local drug delivery has advantages over systemic due to lower immune related toxicity and better tissue distribution. However, due to the small pore sizes, the stratum corneum offers a significant barrier especially for the delivery of macromolecules such as siRNA and plasmid DNA (pDNA) [15]. In addition to pass the SC, for melanoma therapy, the BRAF siRNA molecule needs to permeate the viable epidermis and localize in the basal cells of the epidermis where melanocytes reside. For topical treatment of skin diseases, it is important for a drug to not only permeate through the skin layers and reach the targeted cells, but also to deposit in the skin layers. Drug permeation through the stratum corneum depends upon the interaction between the skin and drug thus both drug and the skin (membrane) properties are two main contributors that determine depth of drug penetration and deposition [16].

The purpose of our studies was to formulate an edge-activated liposomal system complex to siRNA which can “squeeze” itself between small pores of stratum corneum and deposit the drug in the basal epidermis. We selected melanoma as a skin disease

model and the purpose of the study was to design a system that may be able to deliver the siRNA to the melanocytes that reside in the basal epidermis. To achieve this objective, we initially compared skin permeability properties using two synthetic membranes. In this part of the studies we compared permeation of lipophilic and hydrophilic compounds through human cadaver skin, cellulose acetate and Strat-M membranes. In the next step, we compared properties of two antimicrobial agents that not only can permeate through the skin layers but also deposit in it. Finally, we formulated wide ranges of liposomal systems complexed with siRNA and characterized them in terms of size, charge, and charge neutralization. Afterward, skin permeation and deposition of each formulation was tested using human cadaver skin. The ability of permeated siRNA in terms of cellular internalization, cytotoxicity, and bioactivity was examined using human melanoma cells. In the last step, the liposomal system was formulated in a hydrogel and the permeation of the active through human cadaver skin was tested *in vitro*. In summary, this project introduced a novel system that allowed siRNA to permeate through human skin and deposit in the basal epidermis to efficiently deliver its cargo to the targeted skin cells.

Chapter 2

Topical siRNA Delivery: Challenges and Prospects

Development of small molecules that selectively target components inside cells has revolutionized treatment of cancer, inflammatory diseases, and other chronic disorders. One of these technologies focuses on mechanism of RNA interference (RNAi).

Generally, RNAi is a regulatory mechanism in eukaryotic cells. In this mechanism, short doule stranded RNAs (dsRNAs) are applied by eukaryotic cells to control gene activity through RNA degradation. Exogenously introduced dsRNA into cells is processed by a dicer which then yields to 21-23 base pair RNA fragments. These fragments are named small interfering RNA (siRNA). The mechanism of siRNA in silencing expression of a gene has 2 steps. First, RNA Inducing Silencing Complex (RISC) forms and unwinds double stranded siRNA into two single stranded RNA named as guide and passenger strand. The passenger strand is degraded and the guide strand which is now incorporated into RISC (mature-RISC) is paired with complementary sequence in the targeted mRNA molecule. This pairing leads to the second step in which the mRNA molecule is cleaved by the catalytic component of RISC [17] (**Figure 2.1**).

The direct introduction of synthetic siRNAs to cells is a potent strategy of RNAi. In addition, chemical modification introduced to siRNA can increase their stability, efficiency and reduce off-target effects and hence related immunotoxicity effects [18]. Targeted gene suppression by siRNA is a novel technique that has shown promising results in both preclinical and clinical trials [19, 20]. For treatment of skin disorders, topical route has priority to the systemic one because it serves better tissue distribution, less systemic toxicity, and ease of accessibility [21]. However, permeation of siRNA through skin layers is the major technical challenge due to the skin barriers.

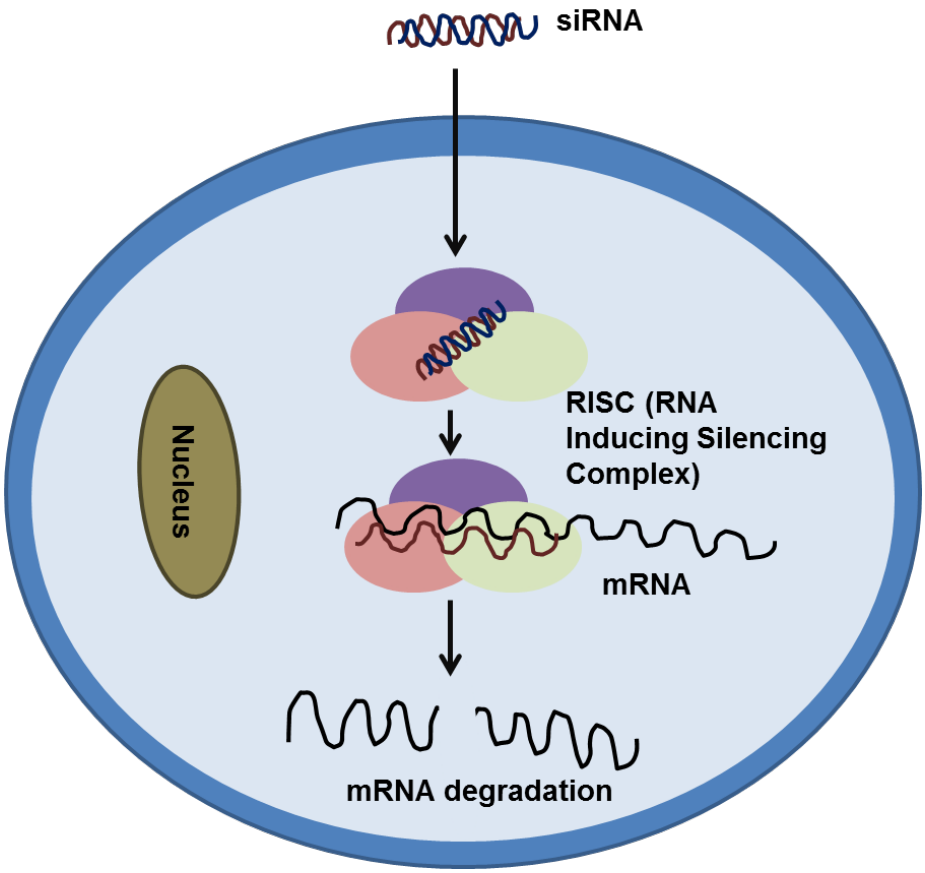

Figure 2.1: The mechanism of siRNA. This figure shows how siRNA silence expression of a gene at RNA level.

Basically, the action site of siRNA is cell cytoplasm [22]. Therefore, siRNA needs to permeate through the SC and other skin layers in order to internalize a skin cell. Naked siRNA is a negatively charged macromolecule with the average molecular weight of 13,300 g/mol. Hence, it cannot permeate through the SC and viable epidermis passively. On the other hand, siRNA is chemically labile and can be easily hydrolyzed by nucleases [23]. Therefore, for topical delivery purposes, carriers are needed which can protect siRNA from environmental hydrolysis, pass it through the skin barrier, and to deliver it to the targeted cells. During the past decades scientists have attempted to develop delivery

strategies to overcome skin barriers in order to take advantage of potential benefits of siRNA in the treatment of skin disorders [24].

2.1. Procedures to Overcome the Skin Barriers

For both transdermal and topical drug delivery there are different strategies to bypass skin barriers. Generally, these technologies can be divided into two main categories of invasive and non-invasive techniques. In the former techniques, hypodermic needles are used to deliver macromolecules into the skin. However, this technique can produce pain, infection, and requires professional assistance [20]. As a result of these drawbacks, non-invasive techniques for transdermal and topical delivery attract more attention. In this approach, microneedles and nanomedicine are the most popular systems that can be applied for skin diseases.

2.1.1. Microneedles

Microneedles (MNs) consist of thousands of microarrays with the height between 25-2000µm in different shapes. Because of their small size, MNs have been shown to penetrate into the SC and through the epidermis without reaching the nerves and blood vessels in the dermis. Therefore, small and large molecules can be delivered into the skin layers with no pain [25]. Overall, four different types of MNs are designed to deliver molecules into the skin. 1) The skin surface is mechanically pierced using solid MNs. 2) The solid MNs are coated with the particles containing the pharmaceutical active. 3) The molecules are encapsulated in polymeric biodegradable MNs. 4) Hallow MNs that are designed for injection [26-29]. (**Figure 2.2**).

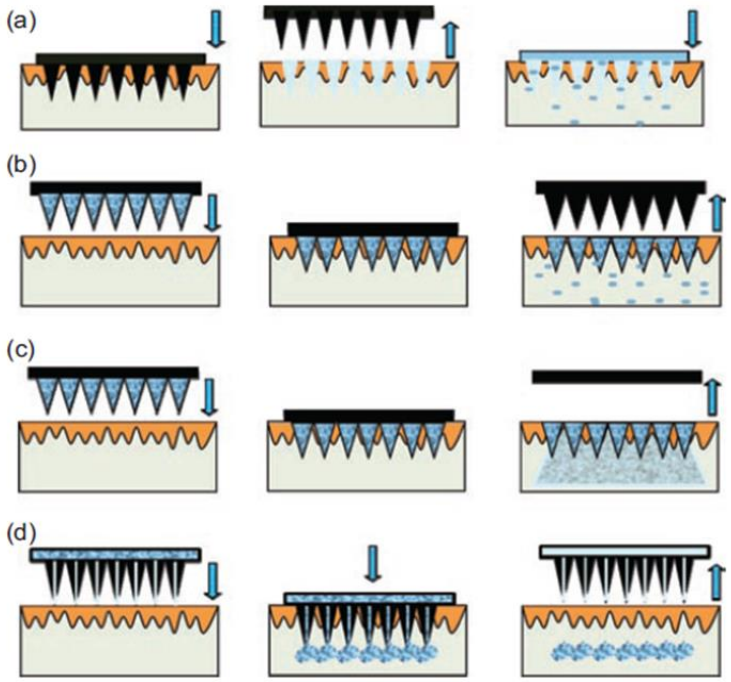

Figure 2.2: Different types of microneedles. Four types of MNs are designed for transdermal drug delivery. (a) Solid MNs. (b) Coated MNs. (c) Encapsulated nanoparticles in biodegradable MNs. (d) Hallow MNs for injection. The figure is adapted from Drug Delivery, 2010; 17(4): 187–207.

Recently, Gonzalez-Gonzalez et al. (2010) loaded 160-320ng Accell modified self-delivery siRNA into polymeric (polyvinyl alcohol) microneedle and evaluated the efficacy of the system in transgenic mouse model which expresses green fluorescent protein (GFP) in upper epidermis. The *in vivo* studies revealed a successful delivery of the siRNA into the skin cells in a sustained fashion and the system could significantly knockdown the expression of the targeted protein compared to the non-targeting siRNA [30]. In another similar study, Chong et al. (2013) designed a microneedle device for delivery of lamin A/C siRNA. In this study, the steel microneedle arrays were coated

with 40 µg Accell siRNA per array. This study showed that the designed MNs could deliver larger amount of siRNA into the upper region of epidermis and knockdown the expression of GFP in the transgenic mouse model. Chong et al concluded that the materials and preparation methods of MNs are important in the loading capacity of siRNA [31].

Microneedles are very novel and interesting techniques and show promising potential for topical siRNA delivery. However, the major drawback of this technique is that the needles need to be firm enough to pierce the skin and the polymeric and biodegradable needles are not strong enough. Another issue is that if it breaks during the application, drug leakage or missed dose may happen. Breaking of a needle inside the skin may cause inflammatory responses [25]. Therefore, safety of microneedles is a missing part that needs to be addressed in future studies.

2.1.2. Nanocarriers

To develop optimized topical delivery of nanoparticle, the interaction of nanoparticles with the skin needs to be understood. Generally, nanoparticles can penetrate into the skin via intercellular, intracellular, and transappendageal pathways. Physicochemical properties of nanoparticles such as size, surface charge, and degree of hydrophobicity can greatly influence the skin diffusion efficiency [32]. Typically, nanocarriers that are fabricated for topical delivery of nucleic acids can be complex with siRNA via electrostatic charges (e.g. cationic liposomes) or conjugate with it in a chemical reaction (e.g. cell penetrating peptides) [22]. In this part we will describe skin penetrating peptides

techniques, carbon nanotubes and lipid based delivery systems as the nanoparticulate systems with significant contribution in topical siRNA delivery.

2.1.2.1. Skin Penetrating Peptides

Skin penetrating peptides (SPPs) are relatively a new strategy that enables noninvasive delivery of macromolecules into the skin. SPPs are mostly short cationic peptides that can either complex siRNA or conjugate with it and deliver it into the skin cells. In 2011 Uchida et al. formulated Tat/siRNA and AT1002/siRNA complexes with size of 70nm and surface charge of +4mV. These complexes were applied to target atopic dermatitis (AD) disorder. AT1002 peptide is a tight junction modulator that reversibly increases paracellular transport of molecules and Tat is a cell penetrating peptide which proposed to be applicable for transdermal siRNA enhancer. This study was conducted *in vitro* on keratinocytes and *in vivo* on ICR mouse model to investigate the efficacy of the complexes to penetrate into the skin. Their studies suggest that the complexes diffused into the skin via either paracellular pathway or hair follicles [33]. In this study, before applying the formulation on mice skin, the SC was removed by tape striping technique in order to mimic AD condition. In AD the SC is disrupted and therefore skin permeability elevates. Therefore, the potential advantage of this delivery system for other skin disorders needs to be studied more. In 2011 Mitrogotri et al. developed new class of SPPs using phage display technique for delivery of siRNA. By using Franz diffusion technique the peptides that showed higher skin permeation were screened and then conjugated with siRNA and applied on balb/c mouse model. They named this new class of SPPs as SPACE (Skin Penetrating and Cell Entering Peptides [34]. Further in 2015, they

suggested that the SPACE internalize into the SC by interacting with the SC keratins and changing the secondary structure of the keratins. This change widens SC transcellular pathways and increases the SPPs skin partitioning. It is also proposed that the SPPs can permeate through viable epidermis with the same mechanism. In their studies they showed that this effect on skin integrity is negligible and has minimal skin cytotoxicity and irritation potential and therefore has a potential for delivery of macromolecules into the human skin [35]. Although this delivery system is a novel technique and the results seem promising, literature show that upon complexation with siRNA, cationic charge of the peptide shifts and this changing in the surface charge reduces their ability to internalize the cell membrane. Therefore, higher concentration of the peptides should be applied to obtain the desired cell penetrating ability which may increase cell toxicity and skin irritation due to an increase in positive charge concentration.

2.1.2.2. Carbon Nanotubes (CNT)

In the family of nanomolecules, CNTs have arisen as an alternative and efficient tool for drug delivery. CNTs are “nano-needles” that can penetrate into cells via a diffusion like mechanism. Moreover, they can be functionalized with drugs, proteins, and nucleic acid and deliver their cargo into targeted cells. CNTs can be functionalized both covalently and non-covalently for drug delivery [36-39]. For example, in 2010 Wu et al. fabricated a programmable CNT device for the transdermal delivery of nicotine. The CNTs were then functionalized with negatively charged dye molecules with four sulfonate groups in order to increase electroosmosis efficiency of the CNTs so that the device will determine the amount of counter ions absorbed to pump neutral molecules

(e.g. nicotine). The in vitro results of this study showed that the system could effectively deliver nicotine through the skin into the saline receptor [40]. For topical siRNA delivery using CNTs, Siu et al. in 2014, fabricated single-walled carbon nanotubes (SWCNTs) for topical delivery of BRAF siRNA. The SWCNTs were functionalized non- covalently with succinated polyethyleimine (PEI-SA) and complexed with fluorescently labeled BRAF siRNA for melanoma therapy. The particles had a length of approximately 1µm with strong positive surface charge ranging 40-60mV. The ability of the system to permeate though the skin was studied on CD-1 mouse model and then the efficiency of the system to knockdown the expression of BRAF gene was studied on C57BL/6 mice bearing melanoma. The results have suggested that the nanotubes could successfully permeate through the mouse skin and deliver siRNA to melanoma cells [41]. Although the system shows great ability to permeate through the skin and deliver its cargo, the toxicity effects of this system needs to be investigated. Although functionalized CNTs with positive charge can effectively complex siRNA and deliver them into cells, high positively charged molecules can have high toxicity and genotoxicity effects [42].

2.1.2.3. Liquid Crystalline Nanodispersions

Lyotropic liquid crystals are a class of nanodispersions that offer enhanced drug solubility, enhanced skin permeation and controlled drug delivery [43]. By modifying liquid crystals with cationic materials (e.g. polymers, lipids), one can obtain the ability to bond to siRNA via electrostatic interactions and thus condense the siRNA. Vicentini et al. (2013) formulated cationic lyotropic liquid crystal nanodispersion by adding polyethylenimine (PEI) (a common cationic polymer for siRNA delivery) or oleylamine

(OAM) (a cationic lipid) to monoolein based liquid crystalline nanodispersions. The prepared formulations were then used to incorporate 2.5 μM siRNA. The prepared particles had average size of 200nm with hexagonal phase interstices. The surface charge of the particles varied depending on the formulation and ranged between 7.0-32.0mV. The skin permeation ability of the formulations was tested in vitro on pig ear using Franz diffusion cells and the bioactivity of the system to knockdown expression of glyceraldehyde 3-phosphate dehydrogenase (GAPDH) protein model was investigated using hairless mouse model. All the formulations showed increased skin permeation in pig ear and the system successfully showed significant silencing efficiency compared to naked siRNA after 24 and 48hours topical application on the animal model with no significant skin irritation [44]. Although a new system for topical delivery of siRNA, further studies should be pursued to verify whether any changes in the composition of the nanodispersion and siRNA concentration can influence the permeation ability of the system.

2.1.2.4. Lipid Based Delivery Systems

2.1.2.4.1. Conventional Liposomes

Administration of liposomal formulations to enhance topical drug delivery was first presented at FIP 1979 congress [45]. After that, different liposomal formulations have been developed for transdermal drug delivery and even found their way in market [46-49]. The topical administration of conventional liposomes for siRNA is limited due to the size restriction and low stability. To address this issue, Tran et al. (2008) developed a combination therapy using ultrasound and liposomal system. In this study, cationic

liposomes were complexed with dual siRNA for the treatment of melanoma and before applying the liposomal formulations, the skin surface of the animal models were treated with low-frequency ultrasound using a lightweight four-cymbal transducer array. The results revealed that the combination of liposome and ultrasound could significantly increase siRNA delivery to the basal epidermis where the melanocytes exist [14]. Active methods such as iontophoresis, ultrasound, and microwaving can increase topical drug delivery; however, it has a safety issue that decreases simplicity of their application.

2.1.2.4.2. Flexible Liposomes

To improve the passive diffusion of the lipid formulations, Cevc et al. (1992) designed a new class of liposomes that have surfactant or alcohol (edge activator) in their structure. These edge activators enable the liposomes to squeeze themselves through the SC spaces under the influence of epidermal water gradient [50]. This system is used frequently in topical delivery of pharmaceutical actives. For example, Goindi et al. (2014) prepared flexible liposomes by thin film hydration method to deliver levocetirizine, an enanthiomer of cetirizine that is widely used for treating allergies. The ex vivo studies, using Franz diffusion cells and murine model skin, revealed a 17.8 increase in permeation of levocetirizine from the flexible liposomes compared to the conventional ones [51]. Application of flexible liposomes is not limited to small molecules and several studies show efficiency of these systems for topical delivery of macromolecules such as DNA and siRNA. For example, Geusens et al. (2009), for the first time, utilized cationic flexible liposomes for siRNA delivery. The flexible liposomes were formulated using a cationic lipid and sodium cholate as an edge activator and the

efficiency of the system to complex siRNA and knockdown the expression of the targeted protein was tested on primary melanoma cells [52]. In another study by the same group, two deformable cationic liposomes containing two edge activators of alcohol and sodium cholate were formulated and their efficiency to deliver fluorescently labeled siRNA was tested on human skin and their results suggest that the flexible liposomes can pass the siRNA through the SC and deposit on top of the viable epidermis [53]. These finding are interesting for topical siRNA delivery especially for treatment of some skin diseases that involves outer layers of the viable epidermis. However, the optimum formulation of these flexible liposomes for higher skin permeation and cytotoxicity effects of this system on human skin cells are not shown yet and studies in this field are limited. Therefore, more studies and formulation developments should be performed in order to take advantages the potential benefits of topical siRNA delivery.

2.1.2.5. Combination Therapy

Combination therapy is a relatively new approach that has been introduced to improve limitations of delivery systems. In this approach two or more delivery systems are combined together to deliver their cargo to the targeted site in a more efficient manner. For instance, Desai et al. (2013) formulated biodegradable lipid-polymer hybrid nanoparticles for a simultaneous delivery of macromolecules and lipophilic compounds. This hybrid consists of cationic amphiphiles with a cyclic pyrrolidinium head and poly lactic-co-glycolic acid (PLGA). The pyrrolidium has a similar structure to azones and 6-amino hexanoates and hence has a potential for use in topical drug delivery. In addition, the particulate system can be easily formed by self-assembly of negative charges of

PLGA at the core and positively charges of the lipid in the shell. The lipophilic compound can easily be added during the assembly to the suspension and thus be entrapped in the core and anionic siRNA can complex with the cationic shell surface after the assembly. The efficiency of the developed system to permeate and be retained in the skin and co-deliver TNFα siRNA (tumor necrosis factor α) and capsaicin was investigated using *ex vivo* (Franz diffusion technique on rat skin) and *in vivo* (psoriatic mouse model) techniques. The results of this study showed that the hybrid system could successfully penetrate deep into the dermis and the combination therapy of TNFα and capsaicin had a significant synergy on treatment of skin inflammation that could not be achieved by the separate siRNA or capsaicin therapy. In addition, the pyrrolidinium head in the combined delivery nanoparticles could possibly perturb the lipid structure of the stratum corneum and facilitate the penetration of the system into the skin [54].

Lipid-SPACE nanoparticles are another example of combination therapy. In this approach, the skin penetrating peptide conjugated to GAPDH siRNA model was attached covalently to the surface of lipid based delivery system. The prepared particles had an average size of 108nm and surface charge of 49mV. The combined delivery system could significantly increase siRNA permeation into porcine epidermis by 10-fold in comparison to an aqueous solution and significantly enhanced permeation compared to free SPACE-siRNA or lipid-based delivery system. The combined nanoparticulate system could successfully knockdown the expression of GAPDH protein model in Balb/c mouse model. In this system, the positive charge of the lipid group and translocation ability of the penetrating peptide could synergistically enhance skin permeation and cell internalization of the siRNA in a dose dependent manner [55].

2.2. Directions for Future Research

As mentioned above, each technique and delivery system has limitations. To address this issue, combination delivery is introduced as a new approach. In this technique, two or more delivery systems have been assembled to deliver two or more therapeutic molecules. For instance, recently, Kwon et al. (2015) conjugated arginine-6 (R6) a cationic cell penetrating peptide on the surface of liposomes and the system was loaded with an anti-wrinkle compound and applied on the skin of hairless mouse model. Interestingly, the results showed that the toxicity of the system decreased in comparison to R6 CPP. The results revealed that this combined delivery system could diffuse deep into the dermis and significantly increase the expression of the collagen protein. This deep skin permeation with less toxicity could not be achieved by either the liposome or the R6 CPP [56]. Therefore, it seems that combination delivery can be used in future as an effective delivery system for small and large molecules. This system seems safe and simple to use and hence, as market prospective, the combination of these advantages could elevates patient compliance as well.

2.3. Conclusions

Topical delivery of siRNA for the treatment of skin diseases is an attractive route that has many advantages to the systemic one. The stratum corneum and viable epidermis are the most challenging barriers for topical delivery of siRNA. During the past century, many researches have been conducted to develop and optimize delivery systems in order to overcome these barriers. In this regard, microneedles have a potential to deliver siRNA into the skin, but in limited surface area. Among different nano-particulate systems,

flexible liposomes and skin penetrating peptides are relatively new strategies and application of them in pharmaceutical formulations along with siRNA therapy have been increasingly popular because they have a great potential for transdermal delivery.

Chapter 3

Membrane Properties for Permeation Testing: Skin versus Synthetic Membranes

Skin, as the largest organ in human body, provides an attractive route for drug delivery. Transdermal drug delivery has many advantages over oral delivery as it avoids first pass metabolism and provides less fluctuations in plasma drug levels. In addition, it results in good patient compliance with ease of termination of drug delivery. In order to assess rate and extent of absorption of drugs for transdermal delivery, both *in vivo* and *in vitro* models can be utilized. *In vivo* approaches examine both rate and extent of absorption directly in animal models and provides robust results. However, due to ethical and economic considerations, *in vitro* approaches are highly preferred especially at the earlier stages of many drug development studies. . For routine *in vitro* studies of skin drug permeation the Franz diffusion cell is often use diffusion cell [57]. Different membranes can be used in the Franz diffusion cells including human skin (human cadaver, surgical biopsies and skin from cosmetic surgeries), animal skin (for example, pig, rodent skin), as well as synthetic membranes. Among these membranes, human and animal skins are the most preferred due to the fact that these are the closest to in vivo human skin. However, these two models have limitations such as cost and availability of human skin and ethical considerations for use of animal skins. In addition, biological models exhibit high variability (CV=72%) that complicates experimental design, statistical significance, number of replicates required, and the ability to compare with historical data [58-60]. Moreover, biological models have short half-life, special storage requirements, higher costs and safety issues (biohazard) that limit experimental convenience.

In order to eliminate the need for biological membranes in pilot studies, synthetic (artificial) membranes are often used. In most of the artificial membranes, either the aqueous domain (hydrophilic path) or the lipid domain (lipophilic path) of skin is mimicked [61, 62]. However, there is a significant need for a synthetic membrane that could mimic both hydrophilic and lipophilic drug pathways as seen in normal human skin. One of the synthetic membranes that has been used in diffusion studies for the past decade, is cellulose acetate (CA) membrane [63-66]. CA is a simple, porous synthetic membrane for assessing topical formulation performance that acts as a barrier with no rate-limiting property [67]. The limitation of CA as a porous membrane is that it completely does not represent human skin barrier properties. In addition, it may interact with some chemicals in a drug formulation and in consequence show incorrect drug permeability values [68]. One recently introduced synthetic membrane that may predict both lipophilic and hydrophilic drug permeation with better correlation to human skin is Strat-M by EMD Millipore, Danvers, MA (Joshi et al., 2012). Strat-M is a non-animal based membrane for transdermal diffusion testing that is more predictive of diffusion in human skin without lot-to-lot variability, safety and storage limitations. This membrane is composed of multiple layers of polyether sulfone with a very tightly packed surface layer that creates “morphology” resembling that observed in human skin (**Figure 3.1**) [69].

In vitro drug permeation experiments provide many advantages such as high throughput capabilities [70] and precise controllable experimental conditions [71]. The objective of this study was to compare the permeation of several compounds using

human skin in vitro and two synthetic membranes: CA and Strat-M in order to examine whether these artificial membranes can be useful membranes for topical drug delivery testing/ screening studies. To achieve this objective, diclofenac sodium, hydrocortisone, and caffeine were prepared as saturated and non-saturated solutions in propylene glycol. In addition, the permeation of each compound was investigated from a commercially available pharmaceutical product. .

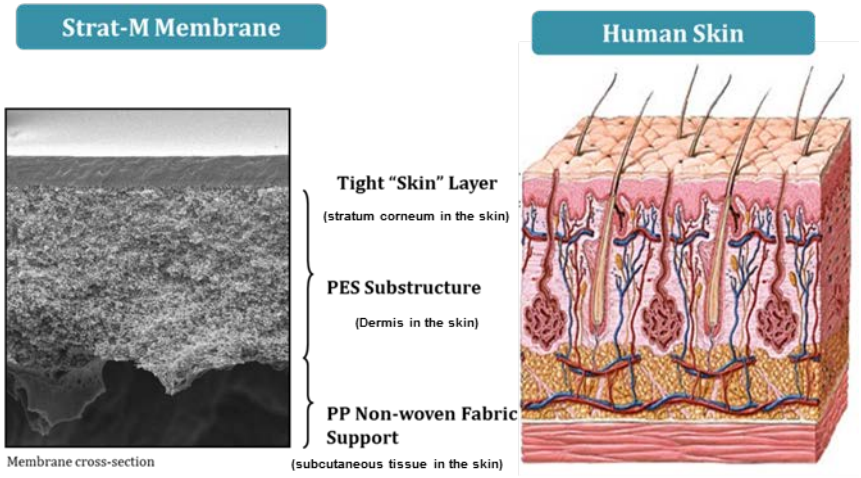

Figure 3.1: Cross section of Strat-M and diagram of human skin. The Strat-M has the "equivalent" of all three layers of human skin and the tight top layer is representative of stratum corneum.

3.1. Materials and Methods

3.1.1. Preparation of Drug Formulations

3.1.1.1. Diclofenac Sodium: 16.64 mg of diclofenac sodium salt powder (Sigma Aldrich, USA) was dissolved in 1 ml of propylene glycol (PG) (ThermoFisher Scientific, NJ, USA) and incubated in a thermostated heat block at 37^{o}C for 48 hours to obtain a

saturated solution [72]. To prepare diclofenac sodium salt 1% solution, 1mg was dissolved in 1ml PG. Voltaren 1% gel was used as the marketed formulation.

3.1.1.2. Hydrocortisone: 20 mg of USP grade hydrocortisone powder (Sigma Aldrich, USA) was dissolved in 1ml PG and incubated at 37^{o}C for 48 hours to obtain a saturated solution. Hydrocortisone solution 1% was prepared in PG. 1% Hydrocortisone Anti-Itch Cream Rite Aid® was used as the marketed formulation.

3.1.1.3. Caffeine: 300mg Caffeine powder (Sigma Aldrich, USA) was dissolved in water and PG then incubated at 37^{o}C for 48 hours to obtain both saturated solution and a dose equal to that found in the marketed formulation (Caffederm®, ThinkGeek,VA, USA). Caffeine 300mg was used as the marketed formulation (Caffederm®, ThinkGeek,VA, USA).

3.1.2. Permeation Assay

The permeation test was conducted using static vertical glass Franz diffusion cells with a donor area of 0.64 cm^2 and a receptor volume of 5.0 mL (Permegear Inc., Hellertown, PA). Dermatomed (~500µm) human cadaver skin samples from posterior leg of three different donors (2 males at the age of 16, 53 and one female at the age of 57) which were obtained from The New York Firefighters Skin Bank (New York, NY, USA), were cut into appropriate size, slowly thawed and then soaked in filtered PBS (pH 7.4) for 30 min. The CA (Whatman GmbH, Pittsburgh, PA, USA) was soaked in PBS for 24 hours before the experiment. The Strat-M membrane (EMD Millipore, MA, USA)was

used immediately with no pretreatment. . Each membrane was then mounted on the Franz diffusion cells with the dermis in human skin and the Strat-Membrane opaque layer facing the receptor. The receptor compartment of each cell was filled with filtered PBS (pH 7.4) and was maintained at 37^{o}C, whereas the surface of the skin was left unoccluded at ambient room temperature. The receptor medium was under synchronous continuous stirring using a magnet stirrer. Prior to applying the formulations, the diffusion cells were allowed to equilibrate for 30 minutes. At time zero, 100 µl of each compound formulation was added to the donor compartment of each Franz diffusion cell and was left uncovered for uniform drying of the formulation on the surface. 500µl of each receptor was collected at time zero, and then every hour for 8 hours. Receptor samples were all analyzed using validated HPLC methods. All the compound formulations were prepared in 6 replicates, and the data are reported as mean ± s.d.

3.1.3. Reverse-phase high performance liquid chromatography (HPLC)

For all measurements, validated HPLC methods were used. The HPLC instrument was Hewlett-Packard 1100 series with UV detector DAD G1315A, and HP Chemstation software version number 32 (Agilent Technologies, CA, USA). The HPLC method of analysis for each compound is provided below:

Diclofenac sodium:

Column: Eclipse XDB-C18. Particle size 5µm. Length: 4.6 x 150mm (Agilent Technologies, CA, USA).

Mobile phase: Acetonitrile: HPLC water/ Trifluoroacetic anhydride (TFA) (60:40) pH 3.0

Flow rate: 1.0 mL/min

Volume of injection: 20µl

Column Temperature: 25^{o}C

Wavelength: 281nm

Stop time: 15 min

Hydrocortisone:

Column: Eclipse XDB-C18. Particle size: 5µm, Length: 4.6 x 250mm (Agilent Technologies, CA, USA).

Mobile phase: Acetonitrile: HPLC water (40:60)

Flow rate: 1.0 mL/min

Volume of injection: 40µl

Column Temperature: 25^{o}C

Wavelength: 242nm

Stop time: 8 min

Caffeine:

Column: Eclipse XDB-C18. Particle size: 5µm, Length: 4.6x250mm (Agilent Technologies, CA, USA).

Mobile phase: Methanol: HPLC water: Acetonitrile (20:70:10)

Flow rate: 1.0 mL/min

Volume of injection: 20µl

Column Temperature: 25^{o}C

Wavelength: 270nm

Stop time: 8 min

(All reagents were HPLC grade and obtained from EMD Millipore, MA, USA).

3.1.4. Data Analysis

To assess the calibration plot for each formulation, dilutions of each compound were prepared by dissolving the compound in its corresponding mobile phase and then dilutions of each compound were analyzed with the relative HPLC method. Then standard calibration curves were prepared for each compound. The cumulative mass of drug permeated through area of each membrane (μg/cm^2) was plotted as a function of time. Each drug concentration value was corrected for progressive dilution using the equation:

$$Qn = \frac{Cn \times V0 + \sum_{i-1}^{n-1} Ci \times V0}{S}$$

Where Cn stands for the drug concentration of the receiver medium at each sampling time, Ci for the drug concentration of the sample, and V0 and Vi stand for the volumes of the receiver solution and the sample, respectively, S for the effective diffusion area [73]. Statistical analysis of the data was performed by employing Anova and Student-t test, with the significance level set at <0.05. Data are reported as mean±s.d. (n=6).

3.2. Results

Selected compounds with varying hydrophilicities were utilized in this experiment in order to compare the permeability of the Strat-M membrane to that of human skin. Among these compounds diclofenac sodium with ClogP (calculated octanol/water partition coefficient) of 4.40 is a lipophilic compound and the two other drugs are hydrophilic with ClogP -0.06 of caffeine and 1.70 of hydrocortisone [74, 75]. Each compound was formulated as a saturated solution in PG providing maximum

thermodynamic drive of the compound across the membranes. Secondly, the permeability (passive) of each of the membranes was tested using formulated compounds as solutions, gels, creams, and as a topical patch. The cumulative drug permeated over 8 hours per membrane area of diclofenac sodium in PG and formulated as a gel is depicted in **Figures 3.2-3.4**. In order to show skin permeability variation that is inherent in a clinical population, skin samples from three different donors were used: two male and one female in different age ranges (from 24-65). The Figure shows that the cumulative drug amounts permeated through the three skin samples and three sets of CA were significantly different from one another ($p<0.05$). Meanwhile, no significant difference was observed between the Strat-M samples. While the permeation trend in the Strat-M membranes is the same as for human skin, the rate of permeation in the Strat-M is significantly higher than that of the skin. However, the Strat-M was able to reproduce skin permeability behavior more than the CA. This observation was more significant in the first three hours for the saturated solution of diclofenac.

In the next step, hydrocortisone was dissolved in PG to either obtain a saturated solution or a 1% solution. The permeation of the drug over 8 hours was observed through human cadaver skin samples and the synthetic membranes. The **Figures 3.5 -3.7** represent permeation comparisons of saturated hydrocortisone as well as the hydrocortisone formulations through human cadaver skin, Strat-M and CA. There was a significant variation between permeability between the data from the skin donors. Interestingly, this high variability could also be seen in CA membranes even though these are not biological membranes. On the other hand, the permeation variation was not

recorded between the Strat-M membranes. The order of the rate of permeation of all formulations of hydrocortisone through human cadaver skin and the two synthetic membranes were: CA>Strat-M>Human skin. In addition, cumulative permeation of hydrocortisone in Strat-M was higher than that of the diclofenac sodium.

Cumulative permeation of saturated caffeine solution in PG and a caffeine patch from the skin, Strat-M and CA is depicted in in **Figures 3.8 and 3.9**. Overall, the permeation of caffeine from the Strat-M was higher than hydrocortisone and diclofenac. A significant variation was seen between the permeability of skin samples and also CA membranes, while no variation was observed in permeability of the Strat-M membranes. The order of permeation values for both saturated caffeine PG solution and the patch formulation were the same for Strat-M and human skin but significantly different for CA. The rate of permeation of caffeine formulations through the membranes was: CA>Strat-M>Human skin.

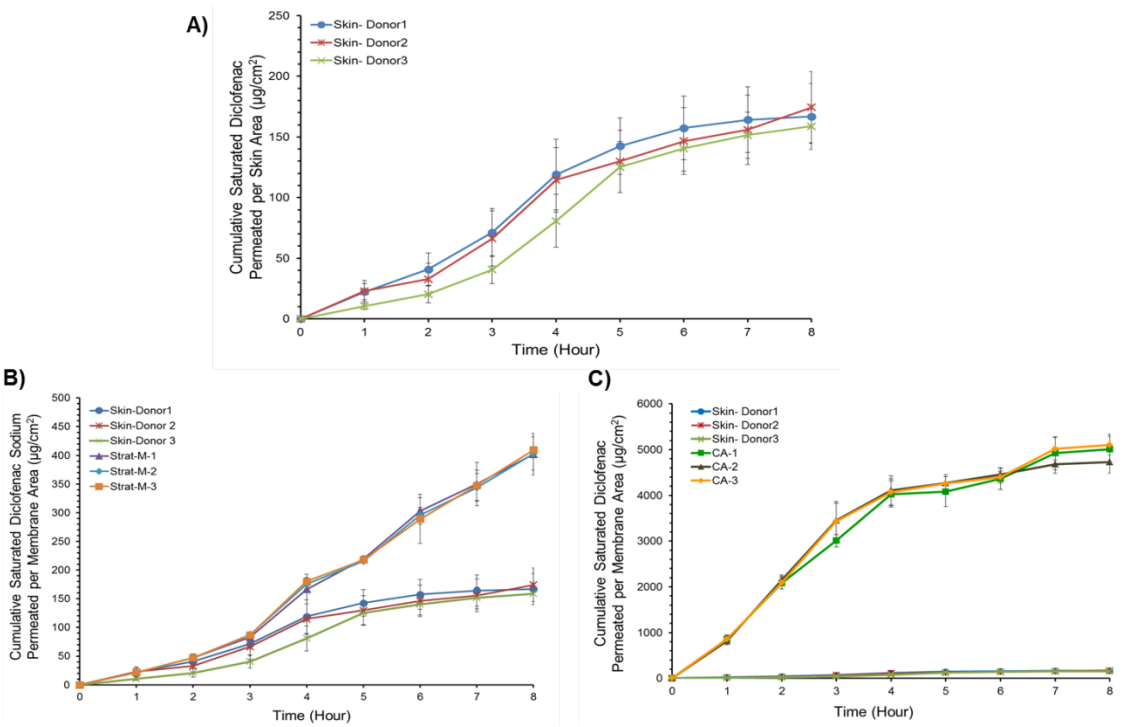

Figure 3.2: Comparison of 8 hour permeation of saturated diclofenac sodium in PG through human cadaver skin samples and synthetic membranes. . A) Human skin; B) Strat-M and human skin; C) CA and human skin. Reported as mean±s.d. (n=6).

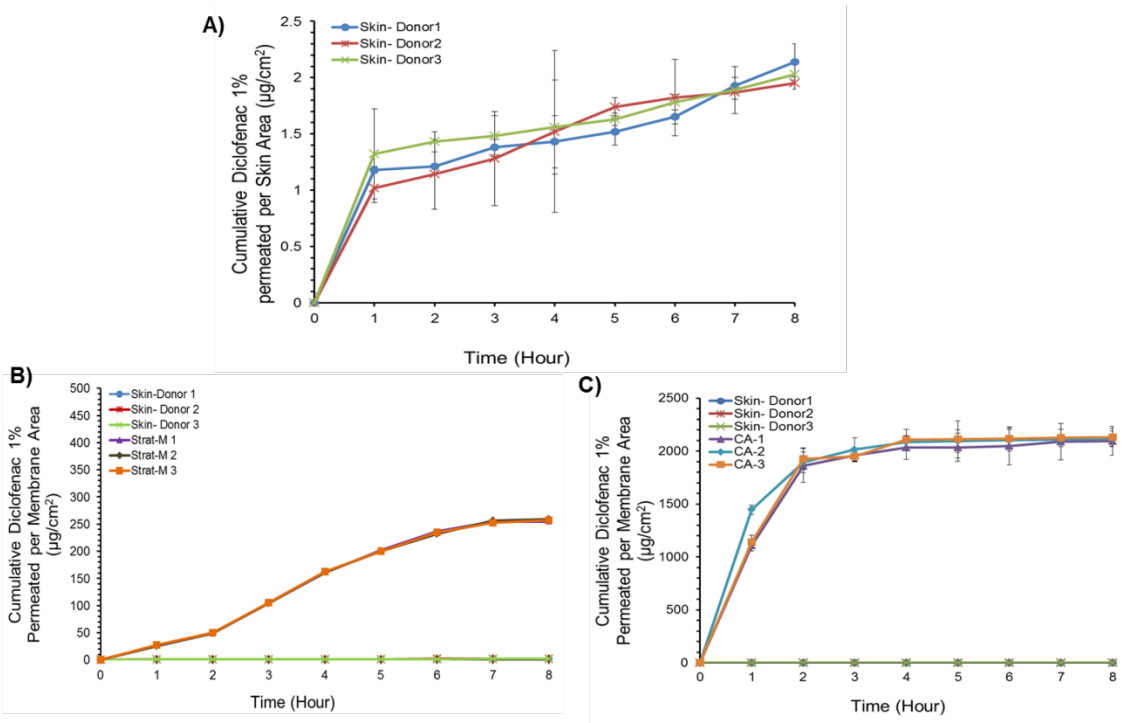

Figure 3.3: Comparison of 8 hour permeation of diclofenac sodium solution 1% in PG through human cadaver skin samples and synthetic membranes. A) Human skin; B) Strat-M and human skin; C) CA and human skin. Reported as mean±s.d. (n=6).

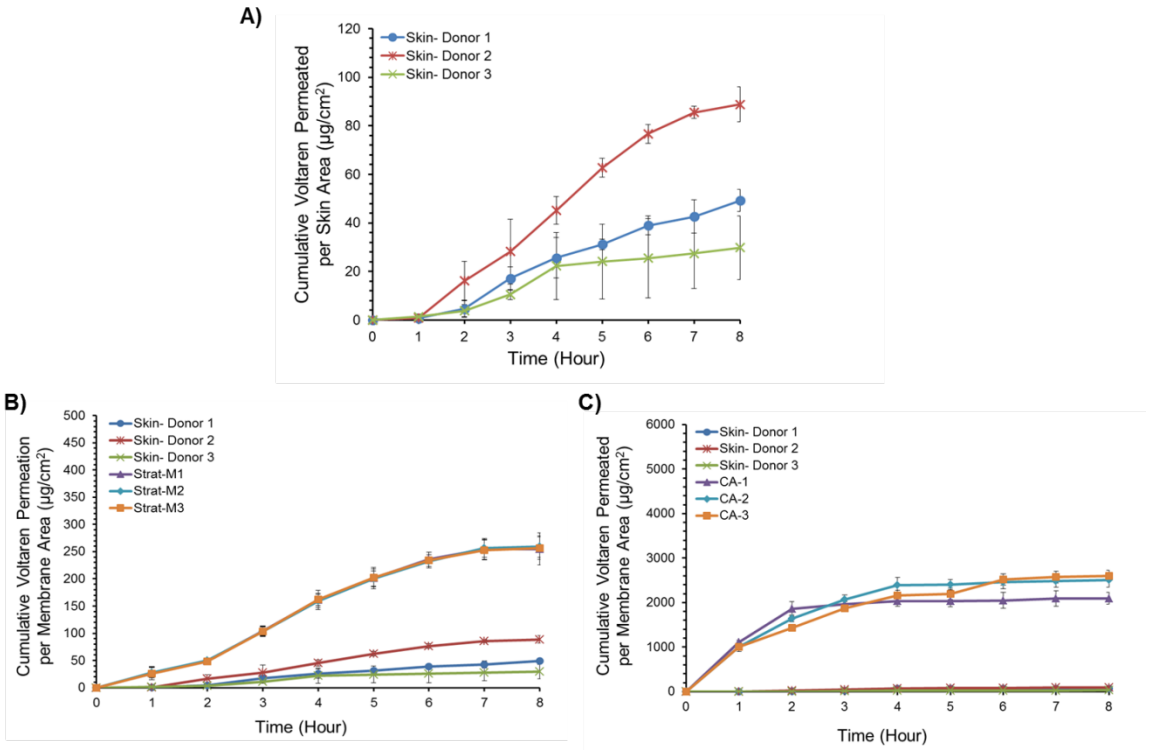

Figure 3.4: Comparison of 8 hour permeation of diclofenac gel (voltaren gel) through human cadaver skin samples and synthetic membranesA) Human skin; B) Strat-M and human skin; C) CA and human skin. Reported as mean±s.d. (n=6).

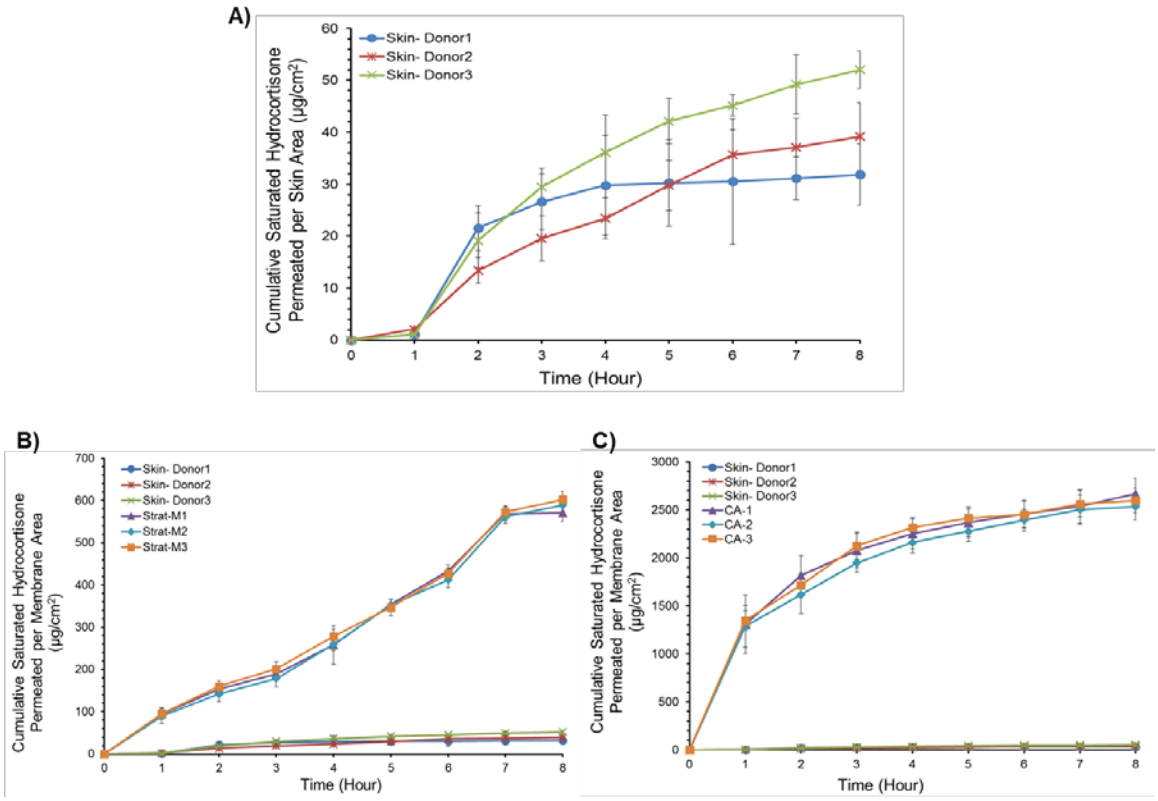

Figure 3.5: Comparison of 8 hour permeation of saturated hydrocortisone in PG through human cadaver skin samples and synthetic membranes. A) Human skin; B) Strat-M and human skin; C) CA and human skin. Reported as mean±s.d. (n=6).

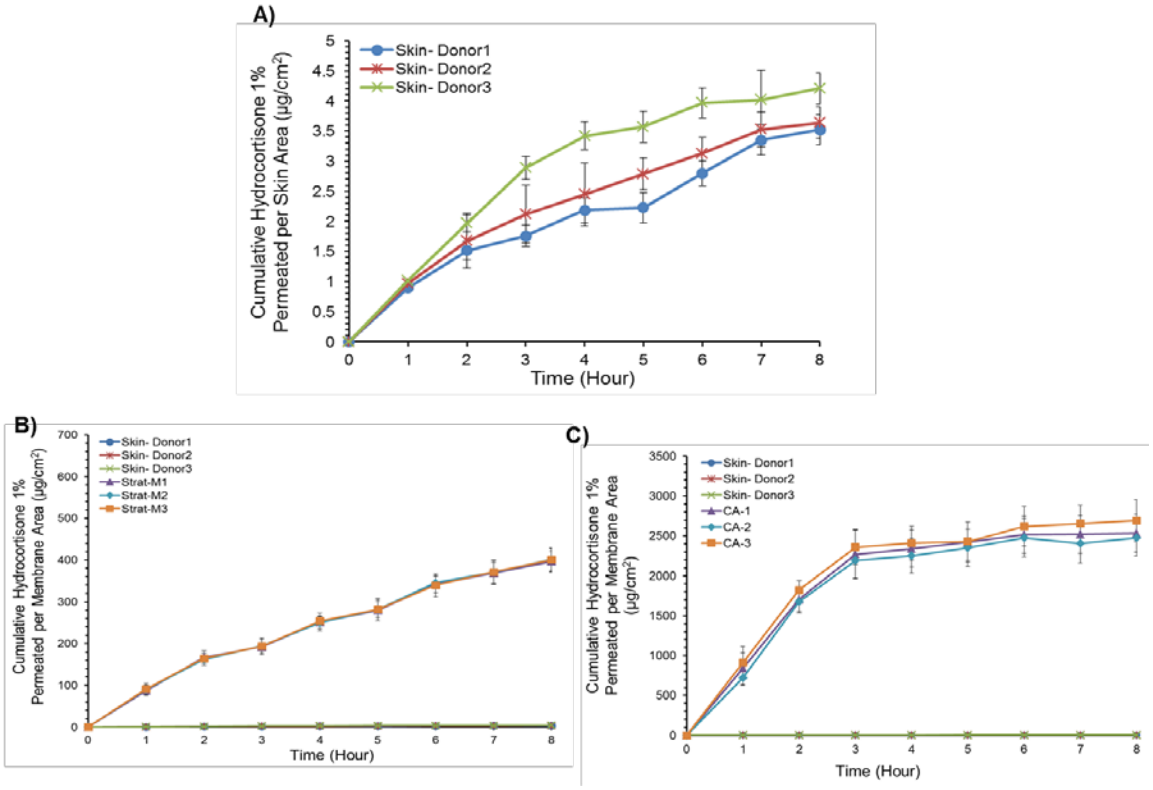

Figure 3.6: Comparison of 8 hour permeation of hydrocortisone solution 1% in PG through human cadaver skin samples and synthetic membranes. A) Human skin; B) Strat-M and human skin; C) CA and human skin. Reported as mean±s.d. (n=6).

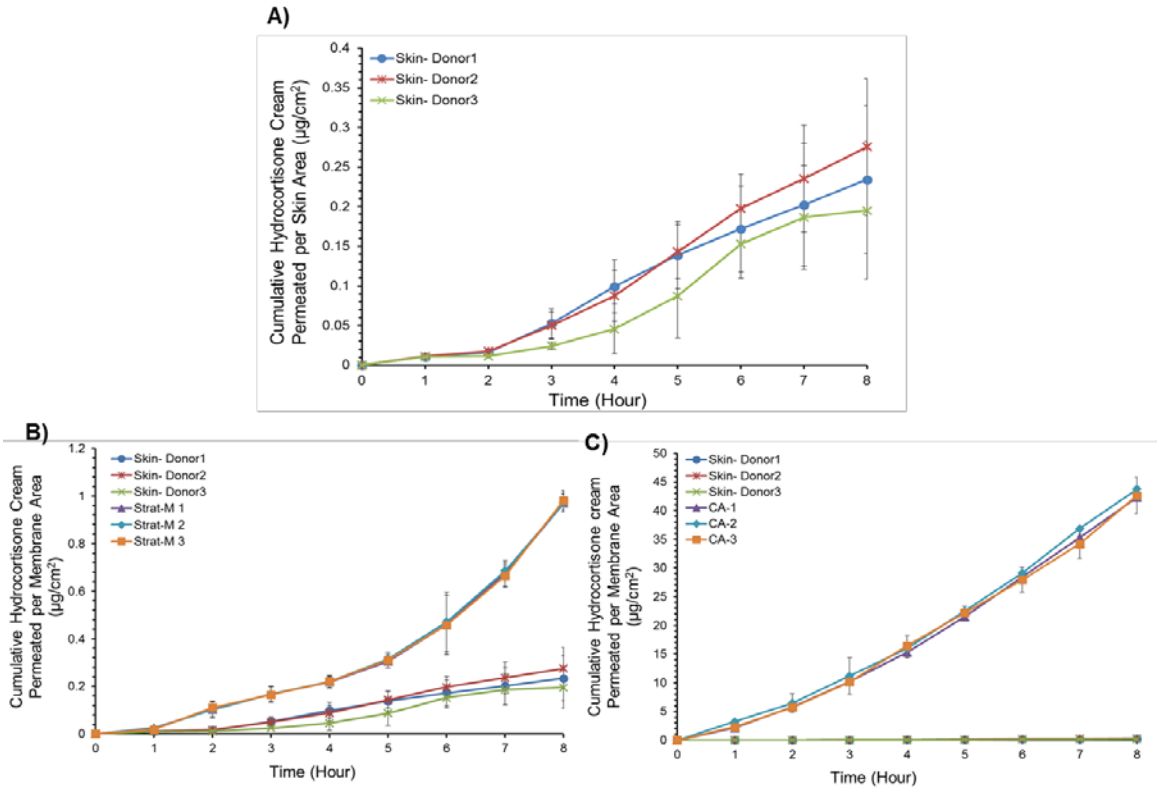

Figure 3.7: Comparison of 8 hour permeation of hydrocortisone cream through human cadaver skin samples and synthetic membranes. A) Human skin; B) Strat-M and human skin; C) CA and human skin. Reported as mean±s.d. (n=6).

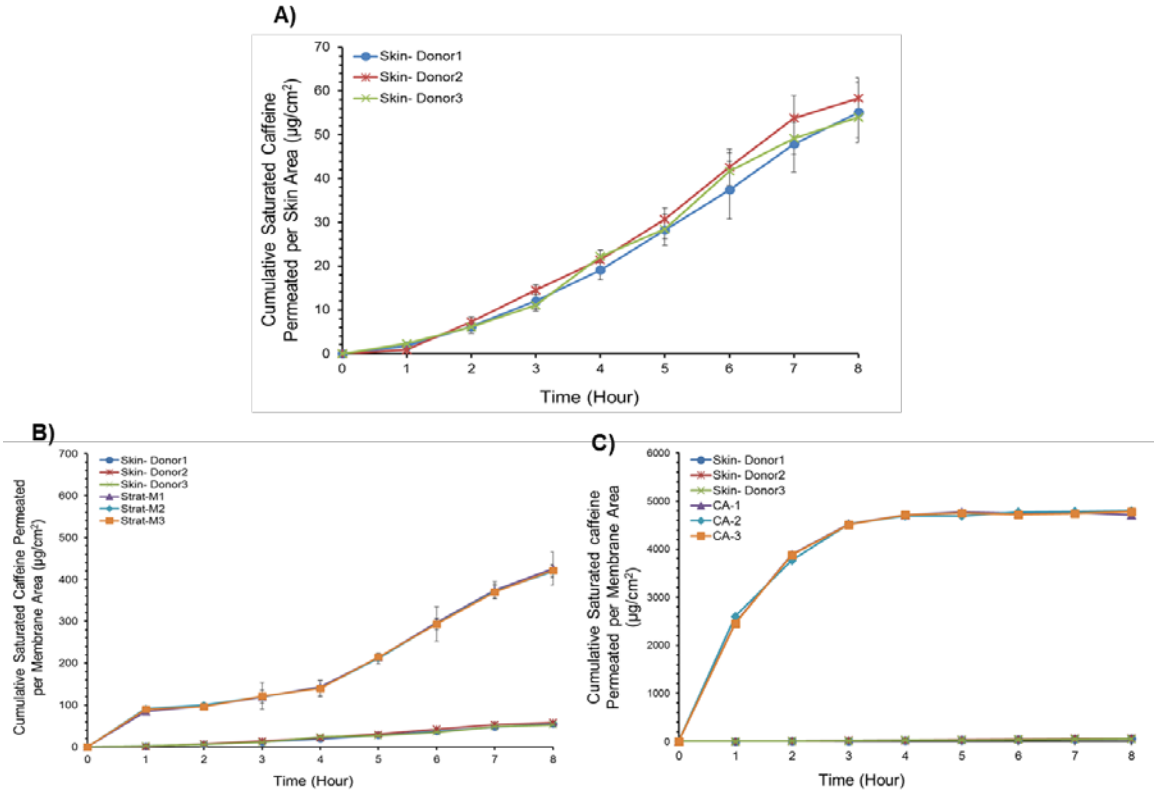

Figure 3.8: Comparison of 8 hour permeation of saturated caffeine in PG through human cadaver skin samples and synthetic membranes. A) Human skin; B) Strat-M and human skin; C) CA and human skin. Reported as mean±s.d. (n=6).

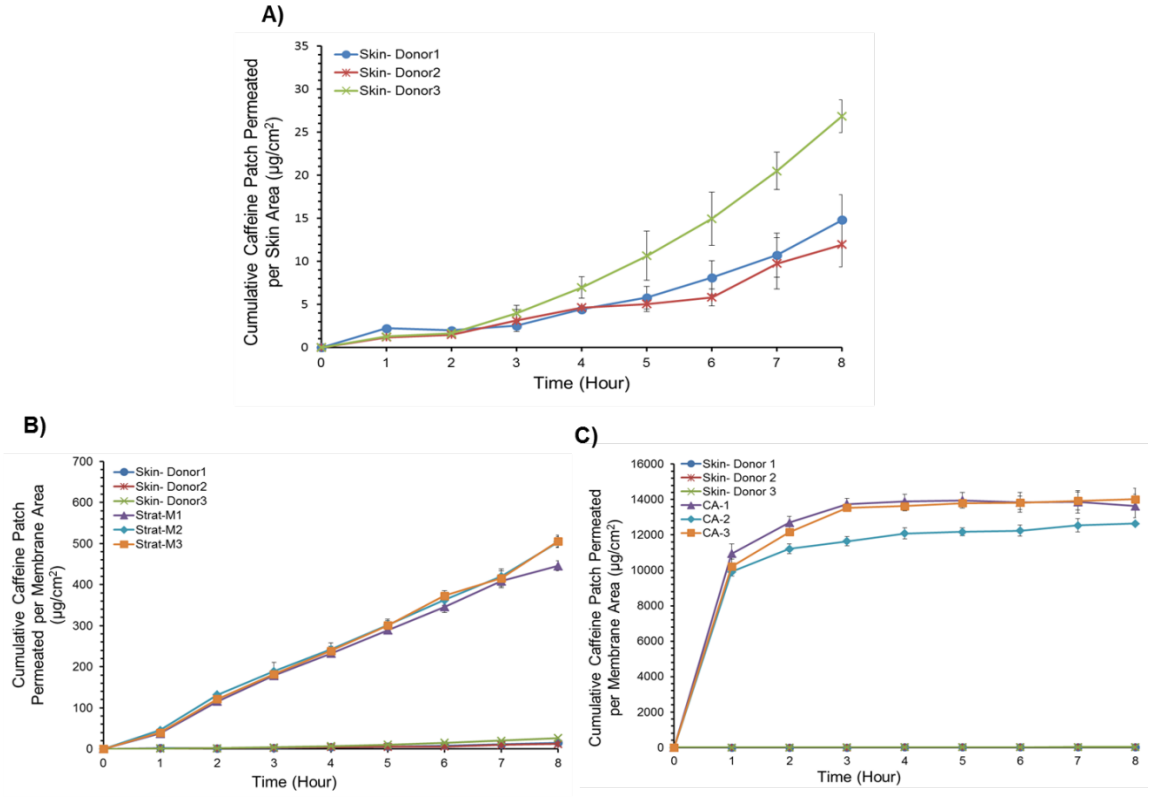

Figure 3.9: Comparison of 8 hour permeation of caffeine patch through human cadaver skin samples and synthetic membranes. A) Human skin; B) Strat-M and human skin; C) CA and human skin. Reported as mean±s.d. (n=6).

3.3. Discussion

Skin is an attractive route for both transdermal and topical (localized) drug delivery. Assessment of permeation of pharmaceutical actives through the skin is an important step during development of drug formulations applied to the skin. Diffusion studies are usually conducted using human or animal skin models such as porcine skin. However, human skin has intra- and inter-lot variability in data as high as 37% and 50%, respectively [76]. In addition, the site of administration (arm, leg, trunk), age, sex and race can influence diffusion of actives in the skin [77]. Poor skin permeation and diffusion variation is often due to the barrier function of the stratum corneum (which consists of heterogeneous dead protein rich corneocytes residing in intercellular lipids) that provides both hydrophilic and lipophilic domains for drug transport. The corneocytes of the stratum corneum are closely packed which makes the pore sizes in the stratum corneum as small as20 nm. This results in the fact that molecules higher than 600 Dalton cannot pass through the stratum corenum passively and this is why the stratum corneum is regarded as the rate limiting step for passive drug diffusion [78-80]. Any artificial membrane used to predict skin absorption should mimic the stratum corneum structural properties as closely as possible. Cellulose acetate is a synthetic, simple and porous membrane that has been used for topical diffusion and release studies for a long time [64]. The limitations of CA is that the pore size of CA is larger than that of human skin which causes higher permeation in comparison to a biological membrane. On the other hand, the Strat-M membrane is an ultrafilteration membrane composed of two layers of polyether sulfone layers that is provides some resistance to drug permeation and below this is a layer of polyolefin that is more open and hence more permeable. These

polymeric layers create a porous structure which is impregnated with blends of synthetic lipids that provides gradient of pore size and diffusivity [71]. In our experiments, we observed that the cumulative permeation of hydrocortisone and caffeine (the hydrophilic compounds) from Strat-M was higher than for diclofenac (the lipophilic compound). This may be related to the permeation routes within the membrane in which the tortuosity of the hydrophilic pathway is lower resulting in higher permeation of hydrophilic compounds in the Strat-M membrane [81]. With all the formulations for the three compounds, the permeation variability of the compounds through Strat-M was less than with human skin and CA which may be related to the homogeneous structure of the synthetic membrane compared to the heterogeneous structure of the stratum corneum of human skin. This homogeneity may obliterate any variation between the replicates. These results are in agreement with a study performed by Uchida et al. (2015) in which the permeation of lipophilic and hydrophilic compounds through Strat-M was compared to human and hairless rat skin [82]. In addition, in their study they showed that the permeation of the compounds through the Strat-M produced correlations with human and hairless rat skin. In our studies, we compared permeation rate of several compounds through skin and two artificial membranes and observed that the permeability of Strat-M was closer to that of skin than that of CA. However, we did not see a significant correlation between Strat-M and human skin. This discrepancy between the observations of Uchida et al. and ours may bedue to the fact that the skin hydration time in our studies was 30 min and 12 hours in the Uchida et al. experiments. The extensive hydration of skin may lead to disruption of the lipid ultrastructure of the stratum corneum and hence result in a permeability increase of the skin. However, shorter hydration time have

negligible effect on the lipidic structure of the stratum corneum [83-85]. This suggests that the pore size of the top layer of the stratum corneum is larger than the stratumcorneum pore size. However, this needs to be investigated in future studies. The dataof this study demonstrate that Strat-M has better correlation to human skin in comparison to cellulose acetate that has been used in past studies. In addition, Strat-Mhas negligible permeation variability between replicates a property which was not observed in human skin and CA membrane. In summary, with such properties Strat-M has potential use for early screening of pharmaceutical dosage forms where for example, higher permeability may be a requirement for moving certain formulations forward for further testing and development.

3.4. Conclusions

Our study data suggest that Strat-M can be applied as an inexpensive, stable and simple membrane to discriminate between the permeation of hydrophilic and lipophilic compounds in early stage diffusion studies for both topical and transdermal formulations. Strat-M requires no pretreatment and its uniform structure eliminates the variability inherent in both skin as well as other polymeric membraes such as cellulose acetate.

Chapter 4

Molecular Properties for Permeability Testing: Skin Deposition of Antimicrobial Agents

The skin is a major organ than protects the body from bacteria and other

A version of this chapter is published in Journal of Controlled Released, 2016: Dorrani M. Garbuzenko O.B. Minko T. Michniak-Kohn B. Development of edge-activated liposomes for siRNA delivery to human basal epidermis for melanoma therapy. J Control Release. 2016; 228: 150-8.

environmental pathogens. In injuries such as burns and trauma, the skin becomes vulnerable to microbial invasion due to the skin's loss of integrity and suppression of local and systemic immunity [86, 87]. As a result, local infection may not only delay the wound healing process, but also can cause systemic infection under severe conditions [88]. The most common Gram-positive bacterial pathogen that colonizes wounds and causes infection is *Staphylococcus aureus (S. aureus).* Topical antibiotics are used to treat skin infection or as prophylaxis to prevent skin from further infection [89].

Mupirocin (Bactroban®, Centany®) is a topical FDA-approved antibiotic that is widely used in treating topical wound infections, especially those caused by Gram-positive multidrug-resistant (MDR) bacteria, such as methicillin-resistant *S. aureus* (MRSA). Mupirocin reversibly binds to bacterial isoleucyl transfer-RNA synthetase and inhibits bacterial protein synthesis. Although not expected [90], high levels of mupirocin resistance have been reported in *S. aureus* and *Staphylococcus epidermidis* strains [91-94]. For example, resistance mutations in the isoleucyl transfer-RNA synthetase gene have been shown to occur with a frequency of $(7.2 \pm 0.9) \times 10^{-8}$ in *S. aureus* 8325-4 [95]. The imposing threat from multidrug resistance highlights an urgent need to develop new classes of antibiotics.

Recently, we identified a guanidinomethyl biaryl compound [compound **13** in reference [96]] as a bactericidal agent with potent activity against MDR bacterial strains, including MRSA. This compound (hereafter denoted as TXA497) is associated with a mutational resistance frequency in *S. aureus* 8325-4 of $(<3.1 \pm 0.8) \times 10^{-9}$ [96]. Thus, in

contrast to mupirocin, TXA497 is associated with a minimal potential for the emergence of mutational resistance in *S. aureus*. TXA497 is a relatively small hydrophobic molecule (**Figure 4.1)** that has the potential to permeate and deposit in skin layers, making it suitable for treating topical wound infections. The objective of this study was to first compare the antibacterial effects of TXA497 and mupirocin against both MRSA and methicillin-sensitive *S. aureus* (MSSA), and then to compare the ability of these agents to permeate and deposit in human skin layers.

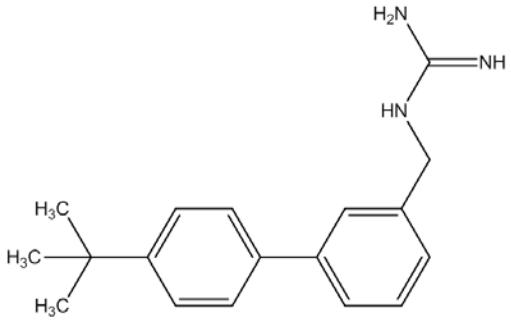

Figure 4.1: Chemical structure of TXA497 (MW = 281.4 g/mol). The indicated ClogP value was calculated using the weighted method (VG = KLOP = PHYS = 1) in the Marvin 5.12 Software Suite (ChemAxon, Ltd.), with Cl^- and Na^+/K^+ concentrations being set at 0.1 mol/dm^3.

4.1. Materials and Methods

4.1.1. Compounds, bacterial strains, and media

TXA497 was synthesized as previously described [96]. Mupirocin and oxacillin were obtained from Sigma-Aldrich, Co. (St. Louis, MO). *S. aureus* 8325-4 and Mu3 were gifts from Dr. Glenn W. Kaatz (John D. Dingell VA Medical Center; Detroit, MI) [97] and Dr. George M. Eliopoulos (Beth Israel Deaconess Medical Center; Boston, MA) [98], respectively. All other *S. aureus* strains (33591 and BAA1708) were obtained from the American Type Culture Collection (ATCC; Manassas, VA). Cation-adjusted Mueller-Hinton (CAMH) broth was obtained from Becton Dickinson and Co. (Franklin Lakes, NJ).

4.1.2. Minimum inhibitory concentration (MIC) assays

MIC assays were conducted in accordance with Clinical and Laboratory Standards Institute (CLSI) guidelines for broth microdilution [99]. Briefly, log-phase *S. aureus* bacteria were added to 96-well microtiter plates (at 5×10^5 CFU/mL) containing two-fold serial dilutions of TXA497 or mupirocin in CAMH broth. Compound concentrations (each concentration being present in duplicate) ranged from 256 to 0.0625 µg/ml. The final volume in each well was 0.1 ml, and the microtiter plates were incubated aerobically for 24 hours at 37 °C. Bacterial growth was then monitored by measuring OD_{600} using a VersaMax® plate reader (Molecular Devices, Inc., Sunnyvale, CA), with the MIC being defined as the lowest compound concentration at which growth was ≥90% inhibited compared to compound-free control. As recommended by CLSI, the CAMH broth was supplemented with 2% NaCl in all MRSA experiments [99].

4.1.3. Preparation of drug formulations

TXA497 was dissolved in propylene glycol (PG) at concentrations of 1.4 and 5.6 mg/ml and vortexed to allow efficient dissolution. Mupirocin was dissolved in PG at a concentration of 5.6 mg/ml. The PG vehicle was used as control in the permeation test for each compound formulation.

4.1.4. *In vitro* skin deposition and permeation assay

The *in vitro* skin permeation study using human cadaver skin was conducted using static vertical glass Franz diffusion cells with a donor area of 0.64 cm^2 and a receptor volume of 5.0 ml (Permegear, Inc., Hellertown, PA). At the time of experiment, dermatomed (500 μm) freshly excised skin samples, which were obtained from The New York Firefighters Skin Bank (New York, NY) from the posterior thigh of a 58 years old male, were cut into appropriately sized pieces, slowly thawed and hydrated in filtered phosphate-buffered saline (PBS) (pH = 7.4), and then mounted onto the Franz diffusion cells. The receptor compartment of each cell was filled with filtered PBS (pH = 7.4) and maintained at 37 °C, and the surface of the skin was open to the environment. The receptor medium was under synchronous continuous stirring using a magnetic stirrer. Prior to applying the compound formulations or the vehicle control, diffusion cells were allowed to equilibrate for 30 minutes. At time zero, 100 μl of each compound formulation was added to the donor compartment of the Franz diffusion cell and left uncovered for uniform drying of the formulation on skin surface. Sink conditions were maintained for both TXA497 and mupirocin. The entire receptor was collected at time

intervals of 0, 3, 6, 12, and 24 hours. All compound formulations were prepared in triplicate, and the data are presented as means ± s.d.

4.1.5. Drug extraction from the skin samples

In order to investigate the amount of deposited compound in the skin at each time point, the skin surface was carefully wiped using Kimwipes and then washed thoroughly 5 times with distilled water to clean the skin surface of any remaining formulation. Prior to compound extraction, the weight of each skin that was in contact with the receptor compartment was recorded. The compound content was recorded as ng of compound per mg of skin. The compounds were extracted into 3 ml of methanol:water [80:20 (v/v)] with skin homogenization. Skin sections were homogenized at 2500 rpm using a PolyTron™ PT 10/35 homogenizer from Kinematica, Inc. (Bohemia, NY) for 15 minutes in the methanol:water. The suspension was centrifuged for 3 minutes at 13,200 rpm, and the resulting supernatant was directly analyzed chromatographically as detailed in the next section.

4.1.6. Reverse-phase high performance liquid chromatography (HPLC)

The HPLC method for analysis of TXA497 was developed in-house, and was validated in terms of linearity, range, limit of detection (LOD), limit of quantification (LOQ), inter-day precision, and intra-day precision. For all HPLC measurements, a reverse-phase SPHER-100 C18 column (Princeton Chromatography, Inc.; Cranbury, NJ) was used on a Shimadzu LC-20AT liquid chromatograph equipped with a Shimadzu SPD-20AV UV/VIS detector set at 254 nm for detection of TXA497 and at 223 nm for

detection of mupirocin. The column size was 150 mm x 4.6 mm with the particle and pore sizes of 5 µm and 100 Å, respectively. A 20 µL sample of each experimental solution was injected and a flow rate of 1 mL/min was applied, along with a gradient of 10% to 90% acetonitrile [containing 0.1% (v/v) trifluoroacetic acid (TFA)] and water in the mobile phase. The total run time was 20 minutes, with the sampling frequency and response time being 2 Hz and 1 second, respectively. Under these conditions, TXA497 eluted approximately 12.2 minutes after sample injection and mupirocin eluted approximately 10.9 minutes after sample injection. Peak areas were determined using the Shimadzu EZStart 7.4 SP3 software package.

4.1.7. Cell proliferation assay

HaCaT human primary keratinocyte cells were cultured at 37 °C (10% CO_2, RH 95%) in Dulbecco's modified eagle medium (DMEM) supplemented with 10% fetal bovine serum (FBS) and 1% penicillin/streptomycin. Cells were then seeded in 96-well plates at a density of 10,000 cells per well. After 24 hours of incubation at 37 °C, the media was changed to include TXA497 at concentrations ranging from 0.3 to 2 µg/ml. DMSO was used as the drug vehicle control. Treated cells were incubated at 37 °C for 24 hours and cell proliferation was measured using the AlamarBlue® metabolic assay kit and protocol (AbD Serotec, Inc.). After addition of the AlamarBlue® reagent and incubation for 3 hours, the fluorescence intensity was measured from 560 to 590 nm (manual gain 100%) using an Infinite® M200 plate reader (Tecan Group, Ltd.). The untreated cell control was used as a measure of 100% viability. All compound formulations were prepared in triplicate, and the data are presented as means ± s.d.

4.1.8. Data analysis

The amount of compound in each experimental sample was determined from the HPLC peak area. Flux (J) was calculated using the following formula: J= M/S-t, where: M is the amount (in µg) of collected compound in the receptor, S is surface area of the skin that was in contact with the receptor (0.64 cm^2) and t is time (in hours). Lag time (t_{lag}) was calculated by extrapolating the steady state of the graph to the *x*-axis, and is reported in hours. Data are presented as means ± s.d. (n=3).

4.2. Results and Discussion

4.2.1. TXA497 is active against mupirocin-resistant MRSA.

The antibacterial activity of TXA497 against *S. aureus* was investigated and compared to that of mupirocin. One MSSA strain (8325-4) and three different MRSA strains (33591, Mu3, and BAA1708) were used in these studies, the results of which are summarized in **Table 4.1**. Inspection of these data reveals that mupirocin is active (MIC = 0.125 µg/ml) against three of the *S. aureus* strains examined (MSSA strain 8325-4 and MRSA strains 33591 and Mu3). A notable exception is MRSA strain BAA1708, which is highly resistant to mupirocin (MIC >256 µg/ml). TXA497 is also active against MSSA strain 8325-4 and MRSA strains 33591 and Mu3, though with a somewhat reduced potency (MIC = 1.0 µg/ml) compared to mupirocin. Significantly, however, TXA497 retains its activity against MRSA strain BAA1708 (MIC = 2.0 µg/ml), which is resistant to mupirocin. Thus, TXA497 remains active against MRSA, even in cases where mupirocin fails due to resistance. As expected, all MRSA strains were resistant (MIC >256 µg/ml) to the control antibiotic oxacillin.

Table 1. Comparison of the Antibacterial Activities of TXA497 and Mupirocin against MSSA and MRSA

Compound	MIC (μg/mL)			
	MSSA 8325-4	MRSA 33591	MRSA Mu3	MRSA BAA1708
TXA497[a]	1.0	1.0	1.0	2.0
Mupirocin	0.125	0.125	0.125	>256
Oxacillin	0.125	>256	>256	>256

[a]MIC values for TXA497 against strains 8325-4, 33591, and Mu3 are taken from reference (Kaul et al., 2012).

Table 4.1: Comparison of the antibacterial activities of TXA497 and mupirocin against MSSA and MRSA.

4.2.2. TXA497 is associated with an enhanced propensity for human skin deposition relative to mupirocin.

We have previously demonstrated that the antibacterial activity of TXA497 is strongly dependent on the hydrophobicity of this compound [96]. These results motivated us to evaluate the ability of the TXA497 to permeate and deposit in human skin. As in the antibacterial studies discussed above, mupirocin was used as a comparator antibiotic in the skin permeation studies. The outermost layer of the skin, the stratum corneum, consists of dead corneocytes, and is the major barrier against topical and transdermal drug delivery [100]. It has frequently been reported that small hydrophobic molecules are ideal compounds for passive topical delivery [101, 102].

Therefore, we designed the next set of experiments to examine whether TXA497 can permeate through the stratum corneum and reach the inner layers of the skin.

For measurement of TXA497 concentration, we first validated an HPLC method with regard to linearity, range, LOD, LOQ, and precision. Linearity was studied in the range of 0.11 to 120 µg/ml, with each concentration being assayed in triplicate. Linearity was observed over the range of 0.23 to 120 µg/ml, with an R^2 value of 0.9992 (**Figure 4.2**). LOD and LOQ values were determined to be 0.036 and 0.12 µg/ml, respectively. Precision is the degree of agreement among individual test results when the method is applied repeatedly to the same or similar samples. The relative standard deviation (RSD %) of six replicates at a concentration of 60 µg/ml, 7.5µg/ml, and 0.93µg/ml were calculated. Based on the observed results (listed in **Table 4.2**), the repeatability (intra-day and inter-day precision) of determined concentrations had RSD values <2%. Using the same approach, the HPLC method for analysis of mupirocin was also validated.

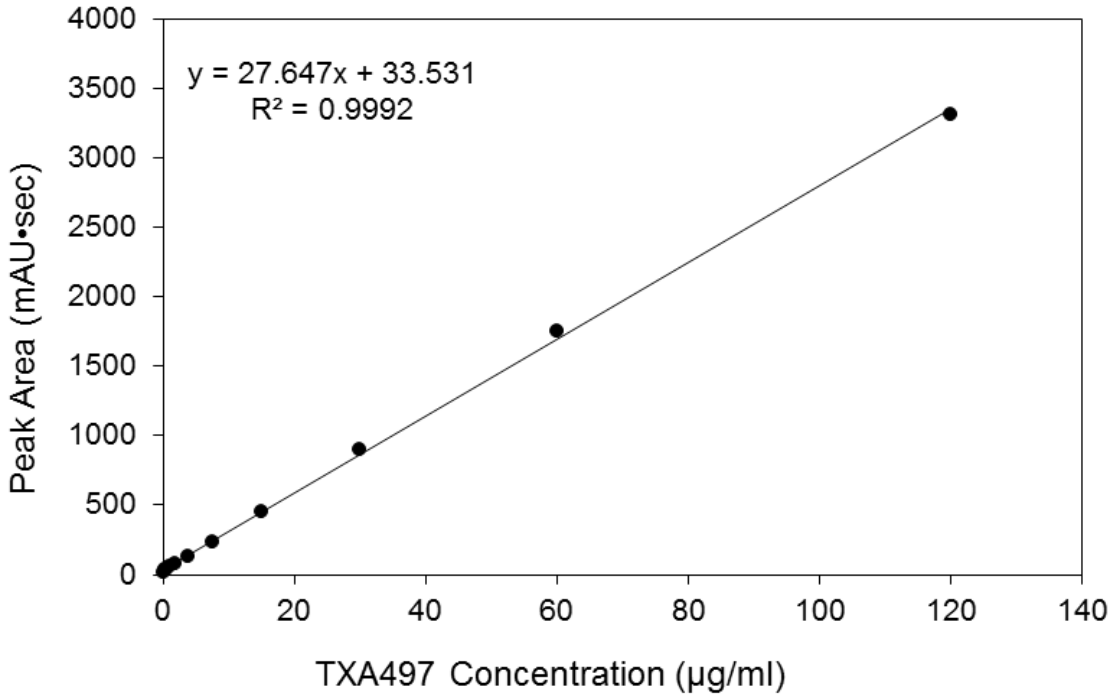

Figure 4.2: Standard curve for quantitation of TXA497 using HPLC.

Table 2. Intra-Day and Inter-Day Precision Analyses of TXA497[a]

TXA497 Concentration (µg/ml)	Intra-Day Analysis		Inter-Day Analysis	
	Response Area (mAU•sec)	RSD (%)	Response Area (mAU•sec)	RSD (%)
60	1771.14 ± 20.74	1.17	1763.26 ± 19.04	1.08
7.5	237.00 ± 2.28	0.96	235.62 ± 3.57	1.51
0.94	53.03 ± 0.15	0.28	52.85 ± 0.24	0.45

[a]Response areas represent the average of 6 injections, and are presented as mean ± standard deviation (SD). RSD denotes the relative standard deviation.

Table 4.2: Intra-day and inter-day precision analysis of TXA497. Each mean represents average of 6 injections. Data is shown as mean ± s.d.

After method validation, we exposed human cadaver skin to TXA497 at concentrations of 1.4 and 5.6 mg/ml and extracted the compound deposited in the skin at different time points ranging from 1 hour to 24 hours. The results demonstrated that TXA497 could be detected in the skin within 1 hour of exposure **(Figure 4.3A).** Furthermore, the rate of compound deposition in the skin was dependent on compound concentration. This observation implies that as the compound concentration in the formulation increases, the rate of compound diffusion through the skin also increases. The basis for this effect can be attributed to Fick's first law, which postulates that the flux (J) is proportional to the amount of material (M) that follows through a section unit (S) over a unit of time (t):

$$J = \frac{dM}{S.dt}$$

Therefore, by keeping the receptor compartment under sink condition and increasing the amount of the compound in the donor compartment, the flux is expected to increase [103].

As noted above, the main barrier for effective topical delivery in skin is the stratum corneum. Depending on the location and level of moisture, the thickness of this skin layer in humans ranges between 10 and 20 μm. The stratum corneum contains lipids and non-viable corneocytes that are cross-linked together by keratin [104]. Molecules <600 Da have been reported to successfully cross this layer with no assistance from physical or

chemical enhancement [78]. TXA497 is a small hydrophobic molecule with a molecular weight of 281.4 Da and is therefore likely to diffuse through the stratum corneum. Furthermore, TXA497 has a lipophilicity (ClogP = 3.96) that should enable the compound to permeate the stratum corneum via the lipoidal route [105]. The small size and lipophilic nature of TXA497 may thus explain why this molecule was able to permeate through the stratum corneum successfully in our study. In addition to the presence of hydrophobic moieties in TXA497, the presence of guanidine group (pK_a 11.60) may also play a significant role in its enhanced skin deposition. The guanidine structure becomes positively charged inside the skin, which has a pH in the range of 5.4 to 5.9. The presence of such a positively charged functionality could help TXA497 permeate and internalize into skin cells better than mupirocin. It has been previously demonstrated that the extent of skin permeation and retention of positively charged molecules is greater than that of negatively charged or neutral molecules, as positively charged molecules can interact with negative surface charges on the cell membranes and become internalized into skin cells [106, 107]. Overall, it is likely that the presence of both hydrophobic and cationic moieties in TXA497 contribute to the contributed to the skin permeation and deposition of the compound.

The results shown in **Figure 4.3B** reveal that, at an equivalent concentration (5.6 mg/ml), TXA497 is associated with a two- to three-fold greater extent of skin deposition than mupirocin. Thus, not only does TXA497 retain activity against mupirocin-resistant MRSA, it also exhibits an enhanced propensity for human skin deposition relative to mupirocin.

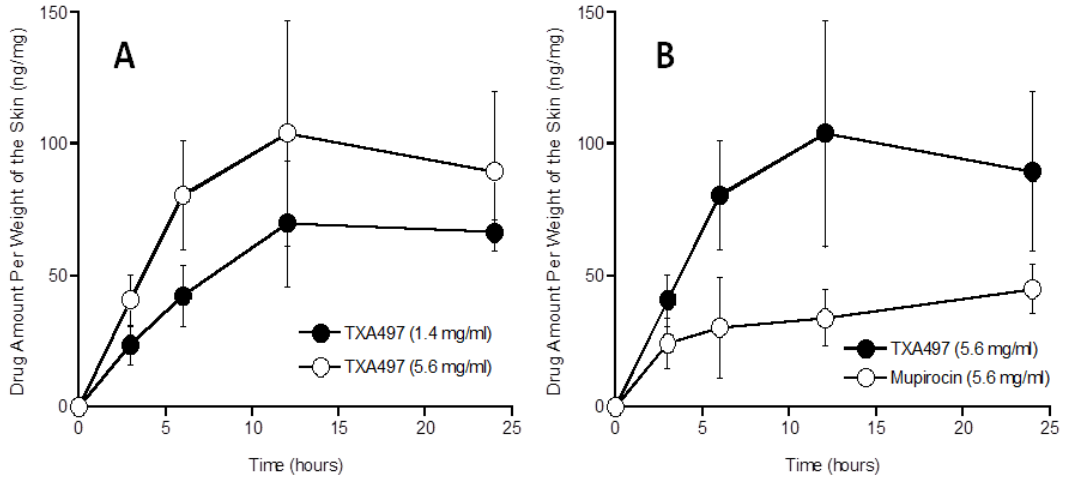

Figure 4.3: Deposition comparison of TXA497 with mupirocin. (A) Concentration dependence of the deposition of TXA497 into human skin. (B) Comparison of the deposition of TXA497 and mupirocin. Skin deposition was studied over 24 hours and is reported per skin weight unit.

4.2.3. Unlike mupirocin, TXA497 does not pass through the entire skin layer.

In the next step, we examined whether TXA497 traversed through the entire skin layer and could be detected in the receptor compartment. The sampling data from the receptor compartment revealed that TXA497 remained in the skin and was undetectable in the receptor compartment.

In striking contrast to TXA497, mupirocin did pass through the entire skin layer (**Figure 4.4**). The calculated lag time for mupirocin to permeate through the entire skin layer was 1.02 hours, with a flux of 1.13±0.62 µg/cm^2.hr. Below the stratum corneum is

a layer of viable epidermal cells that are joined together through tight junctions, leaving little or no intercellular space [108]. Highly lipophilic compounds such as TXA497 (ClogP = 3.96) are expected to slow down when reaching the relatively aqueous environment of the epidermis. As a result, they tend to be retained in this layer and hence concentrate in the skin rather than passing into the systemic circulation [109]. In contrast, less lipophilic molecules like mupirocin (ClogP = 2.45) can easily diffuse through the skin and reach the receptor compartment. Since the purpose of topical drug delivery for treating infection is local therapy, the drug should ideally remain in the skin layers, thereby minimizing absorption into the systemic circulation. Otherwise, significant adverse effects due to systemic toxicity can result, as is the case with many topical steroids [110].

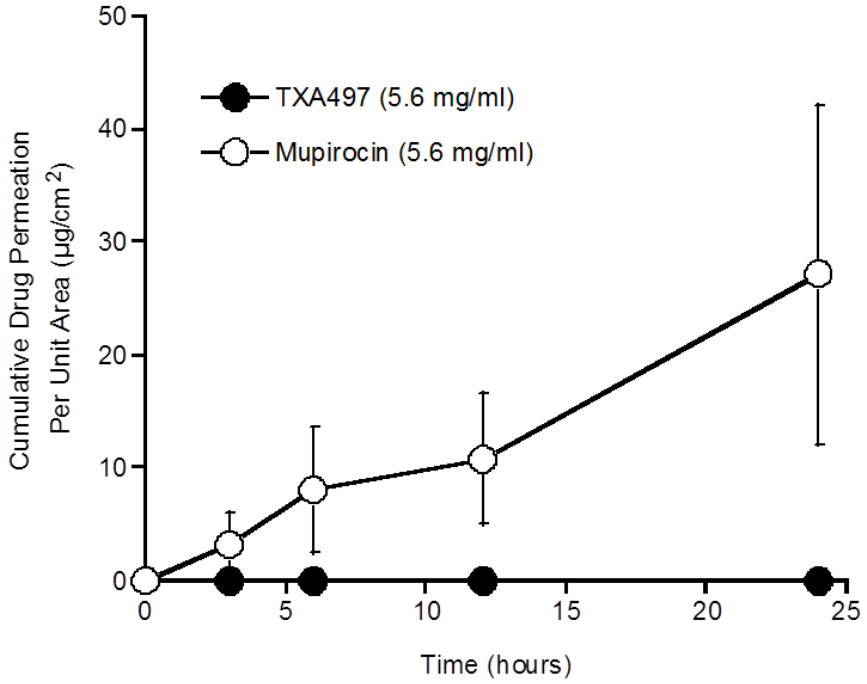

Figure 4.4: Time dependence of TXA497 and mupirocin permeation through the skin into the receptor compartment.

4.2.4. At antibacterial concentrations, TXA497 does not adversely impact the growth of cultured human primary keratinocytes.

Previous reports have indicated that antibacterial concentrations of mupirocin are not toxic to cultured human skin cells [111, 112]. We sought to determine whether the same is true for TXA497. To this end, human epithelial HaCaT cells were exposed to differing concentrations of TXA497 in the range of its antistaphylococcal MICs. Significantly, TXA497 did not adversely impact the growth on HaCaT cells in this concentration range (**Figure 4.5**). Although these preliminary cytotoxicity results for TXA497 are encouraging, additional studies are currently underway to determine how a broader concentration range of the compound formulated as a topical dosage form (e.g., a cream or an ointment) impacts skin cells in both full-layered engineered skin tissue samples as well as *in vivo* animal skin models.

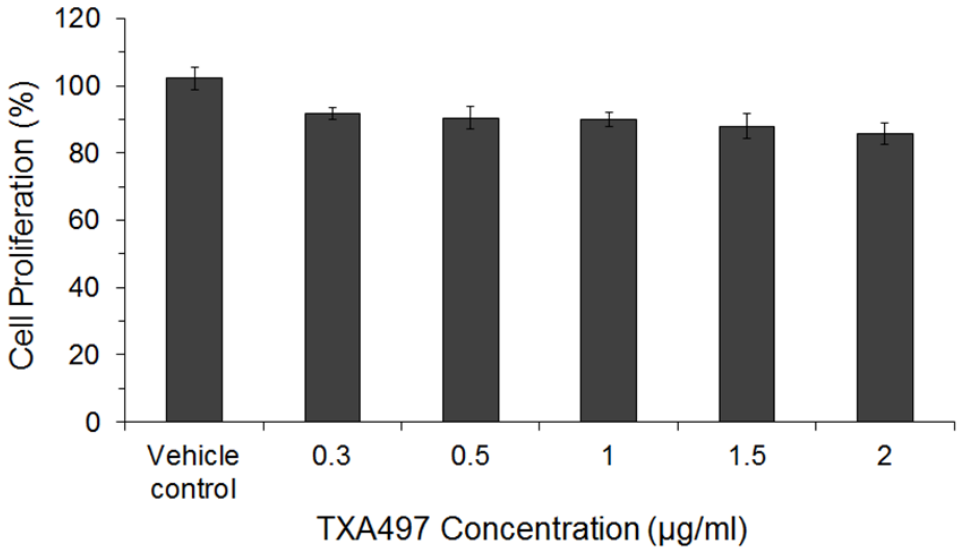

Figure 4.5: Impact of TXA497 treatment on the proliferation of human HaCaT epithelial cells.

4.3. Conclusions

The results of this study demonstrate that TXA497 is able to effectively permeate through the stratum corneum and deposit in human skin. In comparison with mupirocin, TXA497 has both lipophilic and positive groups which help the molecule to not only permeate through the stratum corneum but also deposit in the skin. In addition, it retains antistaphylococcal activity even against mupirocin-resistant strains. Furthermore, TXA497 has no toxicity on human keratinocytes in the concentration range of its antistaphylococcal MICs. By these collective properties we can assume that molecules with lipophilic properties and cationic charged groups may be better candidates for skin permeation and deposition which is an ideal property for topical delivery. Therefore, for the next steps of the studies, liposomal molecules will be formulated with different sizes and surface charges for the topical delivery of siRNA for melanoma therapy.

Chapter 5

Skin Permeation and Deposition of siRNA Using Edge-Activated Liposomal System

A version of this chapter is published in Journal of Controlled Released, 2016: Dorrani M. Garbuzenko O.B. Minko T. Michniak-Kohn B. Development of edge-activated liposomes for siRNA delivery to human basal epidermis for melanoma therapy. J Control Release. 2016; 228: 150-8.

Melanoma is the most malignant form of skin cancer and is a lead cause for the majority of skin cancer deaths worldwide. Over the past decades, some progress has been made in the treatment of melanoma using immunotherapy, chemotherapy and radiotherapy [113]; however, these conventional treatment methods have produced limited success due to significant immune related toxicities, frequent development of drug resistance and poor drug tissue distribution. Therefore, there is a significant need for alternative approaches of drug delivery to the melanoma cells.

One recent successful treatment approach includes the localized drug delivery to melanoma cells via the topical route [52, 114]. For melanoma therapy, delivery of therapeutics to upper layers of the dermis is critical as melanocytes reside in the basal epidermis and on the top of dermis [115]. Therefore, drug molecules need to pass not only through the stratum corneum but also across the viable epidermis in order to reach the melanocytes. Due to the small pore sizes, the stratum corneum is a significant barrier especially for the delivery of macromolecules such as siRNA and plasmid DNA (pDNA) [15]. While a few studies in the past decade have shown progress in delivering macromolecules to the upper epidermis [52, 114], no study has been able to provide a direct evidence to show the effective permeation through stratum corneum and deposition of macromolecules deep in the basal epidermis.

The *objective* of this study was to develop a topical siRNA delivery system that can permeate through the stratum corneum and viable epidermis and efficiently deliver BRAF-targeted siRNA to the basal epidermis where melanoma cells reside. In this study,

we focused on designing a delivery system for topical administration of BRAF-siRNA (v-Raf murine sarcoma viral oncogene homolog B). Molecular analysis of melanoma cells from patients has shown that the majority of the melanocytes contain a mutation in the gene that encodes BRAF protein. Among BRAF mutations, 90% involves a single point mutation that substitutes thymine with adenine at nucleotide 1799 [8]. This mutation in the gene encoding BRAF protein activates the downstream signals of the mitogen-activated protein kinase pathway and ultimately causes an oncogenic increase of melanocytes proliferation and division [10]. Due to the high incidence of mutation in BRAF gene in melanoma cells and increased risk of mortality, we selected the BRAF-siRNA as the model therapeutic for delivery.

Our group has previously shown that cationic moieties should be present in a molecule to effectively permeate through the stratum corneum and deposit in the skin [32]. Therefore, to achieve the objective and in an attempt to overcome the stratum corneum barrier we first prepared a series of cationic liposomal formulations equipped with an edge activator. Then, through the use of quantitative imaging analysis we identified the necessary design parameters for effective permeation of liposome-siRNA complexes (lipoplexes) through the skin layers and deposition in the upper dermis. The liposomal formulations were then examined in terms of their ability to internalize into melanoma cells by quantitative fluorescent microscopy and effective knockdown of BRAF expression by in-cell immunofluorescence assay. In addition, the ability of the lipoplexes to destroy melanoma cells was studied by using WST-1 cell proliferation assay. Finally, we formulated the lipoplexes into carbopol™ 934 gel with different

concentrations and examined the gel formulation in terms of viscoelasticity, release profile, and skin permeation properties.

5.1. Materials and Methods

5.1.1. Preparation of Liposomes

Liposomes were prepared by a solvent dispersion technique as previously described [116]. Briefly, 1,2-dioleoyl-3-trimethylammonium-propane chloride (DOTAP) (Avanti Polar Lipids Inc., AL, USA) at the concentration of 10 mg/ml was dissolved in chloroform (Sigma Aldrich, USA) at room temperature. Using ultra-sonication, sodium cholate (NaChol) (Sigma Aldrich, USA) at the concentration of 10 mg/ml was dissolved in ethanol (>99.5%) (Sigma Aldrich, USA). DOTAP solution was first mixed with NaChol solution at weight:weight (w:w) ratios of 1:4, 1:6, 1:8, and 1:10 (NaChol: DOTAP) and then the solvent was evaporated to a thin film layer using a rotary evaporator. The solvent trace was evaporated by N_2 streaming. The lipid film was hydrated in HEPES buffer (100mM, pH 7.4) for 24 hours at room temperature to let the liposomes assemble. Liposomes were then extruded gradually at room temperature through a polycarbonate filter with 100nm pore size using an extruder (Northern Lipids, Inc., Vancouver, BC, Canada). To obtain fluorescently labeled liposomes for skin permeation and intracellular localization experiments, DOTAP was mixed with green fluorescently labeled DOTAP (DOTAP-NBD) (Avanti Polar Lipids Inc., AL, USA) and the process was repeated as above.

5.1.2. Preparation of Liposome-siRNA Complexes

Lipoplexes were prepared as previously described [117, 118]. Briefly, siRNA was dissolved in nuclease free water. Then, the prepared liposomes were mixed with siRNA solution at w:w ratios of 4:1, 8:1, 12:1 and 16:1 (liposome:siRNA) and incubated at room temperature for 30 min. To prepare, dual labeled lipoplexes, green fluorescently labeled liposomes were mixed with red fluorescently labeled siRNA (siGLO) (Dharmacon Inc., CO, USA).

5.1.3. Particle Size and Zeta Potential Analysis

Liposomes and lipoplexes were prepared as mentioned above and the average size and zeta potential of liposomes before and after complexation with siRNA were measured by dynamic light scattering and laser Doppler Velocimetry (Nano-ZS Zetasizer, Malvern Instruments, U.K), respectively. Three independent batches of liposomes and lipoplexes in HEPES buffer (20 mM, pH 7.4) were prepared and 15 measurements from each sample were made. Data are reported as means±s.d. (n=3).

5.1.4. siRNA Charge Neutralization Study by Gel Retardation Assay

The neutralization of negative charges in siRNA by positively charged liposomes was studied by gel retardation assay. Free siRNA and liposome-siRNA complexes were electrophoresed on 4% agarose gel containing 0.5% ethidium bromide at 150v for 1 hour. The gel was visualized under a UV light using Gel Documentation System 920 (NucleoTech, San Mateo, CA, USA).

5.1.5. Skin Permeation Study

The skin permeation studies of fluorescently labeled lipoplexes were performed using dermatomed freshly excised human cadaver skin from a single donor, the posterior leg of a 54 years old male (New York Firefighters Skin Bank, NY, NY). The skin samples were cut into appropriate sizes and mounted on vertical glass Franz diffusion cells (Permegear, Inc., Hellertown, PA) with a receptor volume of 5.0 ml and donor area of 0.64 cm^2. At the time of the experiment, frozen skin samples were cut into pieces with desired sizes, slowly thawed and hydrated in filtered phosphate buffer saline (PBS) pH=7.4 for 15 minutes. Then, the skin samples were gently mounted on Franz diffusion cells in such a way that the dermis was in contact with the receptor. The receptor compartment of each cell was filled with filtered PBS and maintained at 37ºC under synchronous continuous stirring using a magnetic stirrer, whereas the skin surface temperature was unoccluded and maintained at ambient room temperature. As part of our quality control, before each experiment the skin integrity was tested by measuring the skin conductivity [119]. Skin pieces with integrity below 1.00 mS/cm were considered as “damaged” and replaced with another skin piece with acceptable resistance [120]. Each formulation was studied with 3 replicates. At time zero, 100 µl of each sample containing 3 µg siRNA was added to the donor compartment of Franz diffusion cell using a pipette set. As the control groups, 100 µl of phosphate buffer saline (PBS) with pH 7.4 was added to the donor compartment of Franz diffusion cell (3 replicates). The skin surface was left uncovered for uniform drying of the formulation on skin surface. After 24 hours, the remaining solution was collected and washed thoroughly off the skin surface with distilled water. The entire receptor of the cells was collected and tested for fluorescent intensity using a fluorescence

spectrophotometer (Hitachi Hi-Tech, Tokyo, Japan). All skin samples were collected and studied by fluorescent microscopy.

5.1.6. Fluorescent Microscopy Imaging of Skin Samples

The collected skin samples were immediately fixed with formaldehyde 10% and incubated overnight at 4^{o}C. Then, the samples were frozen in OCT embedding media (Sakura Finetek, CA, USA) and sectioned at a thickness of 20µm using a cryotome (Leica CM1850, Nussloch, Germany). Skin cuts were laid on slides, washed with distilled water and dried at room temperature in the dark. One drop of Fluoromount Aqueous Mounting Medium (Sigma Aldrich, USA) was added to the slide which was then covered with a glass cover slip. Skin samples were imaged using a fluorescent microscope (Olympus, Center Valley, PA, USA) to evaluate the depth of lipoplex permeation. The percentage of lipoplexes in each skin layer was quantified by using ImageJ NIH software (www.imagej.nih.gov). To quantify the concentration of the siGLO that permeated into each skin layer, a standard curve was first plotted by measuring the fluorescent intensity of different concentrations of liposome-siGLO complexes using a fluorescence spectrophotometer F7000 (Hitachi Hi-Tech, Tokyo, Japan). The absorption/emission wavelengths of the instrument were set at 557/570 nm, respectively. Linearity was studied in the range of 0.046- 3.0 µg/100µL of siGLO with each concentration being assayed in triplicate. Linearity was observed in this range with an R^2 value of 0.9929. The stratum corneum layers of the skin samples were first separated from the skin by tape stripping. Then, the epidermis was separated from the dermis mechanically by using a tweezer. The liposome-siGLO complexes in the stratum

corneum, epidermis and dermis were then extracted in PBS pH 7.4 by homogenization (BeadBug™ Microtube Homogenizer, Edison, NJ, USA). The concentration of the permeated siGLO into each layer of the skin was then calculated using the standard curve.

5.1.7. Evaluation of Intracellular Localization of Liposome-siRNA Complexes

To examine the cellular internalization of lipoplexes, UACC-903 melanoma cells were seeded at a density of 2,000 cells per well in a 24-well plate and incubated overnight at 37^{o} C. The next day, green fluorescently labeled liposomes were mixed with 20 µM of siGLO (red fluorescence labeled scrambled siRNA) solution at the w:w ratio of 16:1 (liposome: siGLO) and incubated at room temperature for 30 min before cell transfection. Cells were transfected with the liposome-siGLO complexes for 1 hour at 37^{o}C. After 1 hour incubation, cells were washed 3-4 times using Dulbecco Phosphate Buffer Saline (DPBS) and then the cell nuclei were stained by adding 6µl of DAPI (blue fluorescent dye) (Life Technologies, NY, USA) followed by incubation for another 20 min. Finally, the cells were washed 3-4 times with DPBS and visualized using a fluorescent microscope.

5.1.8. Evaluation of BRAF Expression Knockdown in Melanoma Cells

To investigate the ability of the developed liposomal system to deliver BRAF siRNA into the melanoma cells, an in-cell immunofluorescence technique was used to visualize the expression of BRAF inside the cells. UACC-903 human melanoma cells were seeded at the density of 10,000 cells per well in 96-well plates and incubated at 37^{o}C for 24

hours. Liposomes were then complexed with BRAF siRNA (0.5µg) at the ratio of 16:1 (w:w) for 30 minutes and added to the wells (treatment group). Vehicle (HEPES buffer), empty liposomes, naked BRAF siRNA, liposomes complexed with scrambled siRNA were used as controls. After 24 hours, cells were washed three times with DPBS and then fixed in formaldehyde 10% for 20 min. Cell membranes were permeabilized using a protein-free blocking buffer containing 0.1% Triton 100x. To block the non-specific sites, cells were incubated for 1 hour in a protein free blocking buffer (Thermofisher Scientific Inc., NJ, USA). Cells were first incubated with anti-BRAF primary antibody and then with fluorescently labeled secondary antibody (PierceThermoScientific, IL, USA). After incubation for an appropriate time, cells' nuclei were stained with Hoechst 33258 (blue fluorescent dye) (Life Technologies, NY, USA) and visualized under a fluorescent microscope. The data were analyzed using ImageJ NIH software and reported as means ± s.d. (n=3).

5.1.9. WST-1 Cell Toxicity Assay

UACC-903 human melanoma cells were seeded in 96-well plates at the density of 10,000 cells per well and incubated at 37^{o}C for 24 hours. Liposomes were mixed either with the control scrambled siRNA or BRAF siRNA at different concentrations equivalent to 0.1, 0.2, 0.5 µg. After 30 minutes incubation at room temperature, cells were transfected with lipoplex formulations and incubated at 37^{o}C for 24 hours. WST-1 reagent was added to each well and after 1 hour incubation the absorbance of each sample was measured using a microplate reader at a wavelength of 450nm. The data are reported as means ± s.d. (n=3).

5.1.10. Preparation of Gel

As a vehicle for incorporation of the lipoplexes for topical delivery, two concentrations of gel were prepared as per published procedures (0.5% and 1%). Briefly, Carbopol® 934 (Lubrizol, Cleveland, OH, USA) was dispersed in deionized water by stirring at 800 rpm for 60min. The mixture was then neutralized by dropwise addition of triethanolamine (TEA) 99%. Mixing was continued until a transparent gel was formed and the amount of the base was adjusted to achieve a gel with pH 7.

5.1.11. Incorporation of Lipoplexes into the Gel

The fluorescently labeled lipoplexes (green labeled liposome: red labeled siGLO) were mixed into the carbopol gel by mechanical mixing with a final concentration of lipoplexes being 10% in the gel [121]. Non-labeled lipoplexes (liposome-BRAF siRNA) incorporated into the gel under the same method.

5.1.12. Rheological Measurement

A dynamic mode was used for rheological analysis. Controlled strain of 1% was applied to the samples and all the measurements were carried out at 25^{o}C using on a Kinexus Rotational Rheometer (Malvern, Worcestershire, UK) with parallel-plate geometer of 25mm. The storage (G´) and loss moduli (G″) of the gels were measured from a constant-strain frequency sweep over frequency ranges of 100–0.01 rad s^{-1}.

5.1.13. In vitro Release Study

To study the lipoplex release from the gel, liposomes were labeled with green fluorescently dye and siGLO (the red fluorescent labeled siRNA) was substituted in place of the BRAF siRNA. The agarose barrier technique was used for the release study [122]. Briefly, 500µg of the gel was added to 5mL glass vial and then 200µl agarose 2% was added to the gel that was allowed to harden at room temperature. Afterward, 1mL of receptor solution (PBS pH 7.4) was added on top of the agarose gel. The vial was then reversed and incubated at 37^{o}C for 72 hours. At predetermined time points (0-1-2-4-6-8-12-24-48-72h) 500µL of receptor was collected and the fluorescent intensity of released lipoplexes was measured using fluorescence spectrophotometer F7000 (Hitachi Hi-Tech, Tokyo, Japan). The results are reported as % cumulative released lipoplex in the receptor.

5.1.14. In Vitro Skin Permeation and Imaging

The skin permeation study and imaging was performed as mentioned in the section 2.5 and 2.6. Briefly, 50µg of gel was added on the skin and the receptors and skin samples were collected at 8 and 24h. In this section, 50µg empty gel was used a control. At predetermined time points, the gel formulation was removed from the skin surface and the skin was rinsed off thoroughly with DI water and sectioned with the thickness of 20µm and collected on microscope slides. The skin samples were then imaged using a fluorescent microscope (Olympus, Center Valley, PA, USA) to evaluate the depth of lipoplex permeation.

5.2. Results and Discussion

5.2.1. Particles Size, Zeta Potential and Charge Neutralization Studies

Cationic liposomes were first prepared by using different w:w ratios of DOTAP as the cationic lipid and NaChol as an edge activator ranging from 4:1 to 10:1. NaChol is a surfactant that is known for its ability to open pores in stratum corneum and accelerate permeation of nanoparticles through the skin. NaChol has a pKa of 5.5 which is close to the pH of skin. Geusens et al. (2010) suggested that at this pH NaChol protonation occurs in the lipoplex complex. This protonation tends to be strongly exothermic and this may modulate the skin barrier in favor of the lipoplex permeation [53]. Based on this understanding, we prepared cationic liposomes with different edge activator content in order to carry negatively charged siRNA molecules through the skin. The prepared liposomes were then characterized in terms of size and charge since both of these parameters have significant impact on nanoparticle permeation through the skin. The results of this study showed that as the DOTAP content increased, the size of the liposomes decreased from 120 nm to 60 nm and the surface charge increased from 25 to 37 mV **(Figure 5.1)**. The sizes of liposomes that were prepared with DOTAP:NaChol at ratios of 6:1, 8:1 and 10:1 were statistically in the same range from 60 to 65nm (t-test, $p>0.05$). Formation of lipoplexes was based on the electrostatic interactions between positively charged liposomes and negatively charged siRNA.

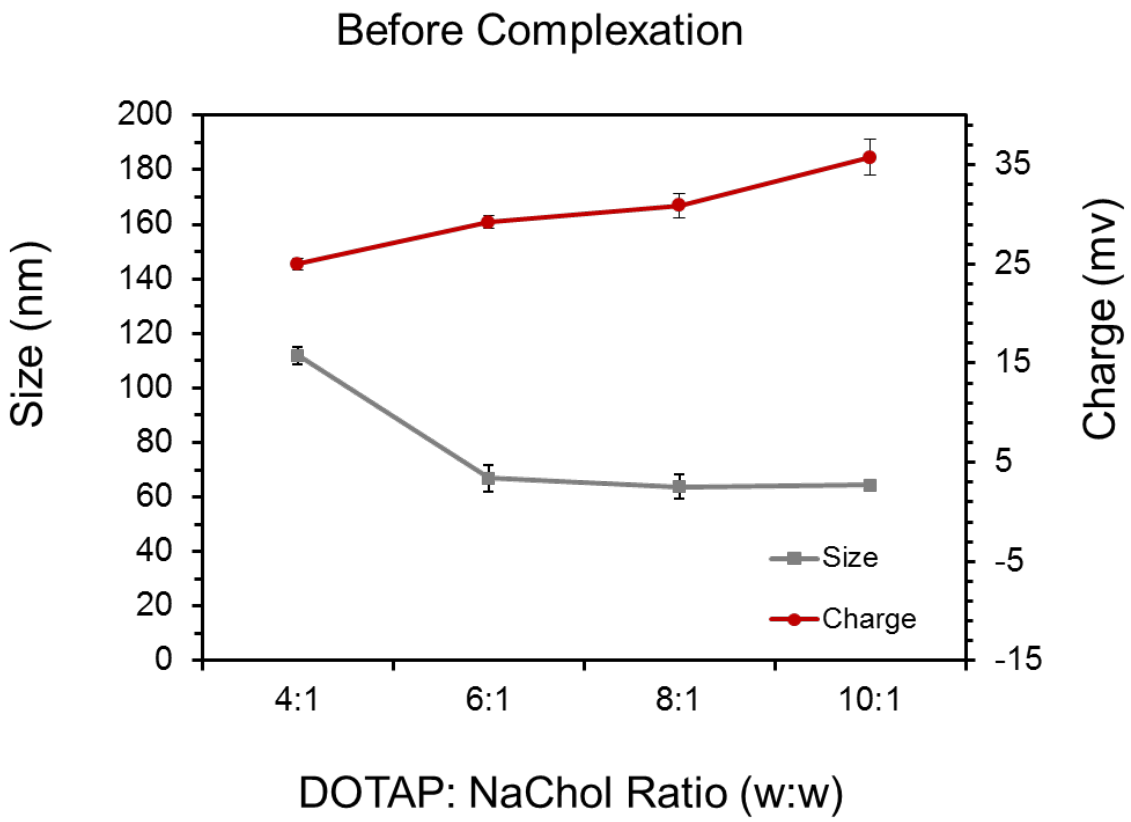

Figure 5.1: Size and zeta potential analysis of empty liposomes at different DOTAP to NaChol ratios ranging from 4:1 to 10:1 (w:w). Data are reported as means ± s.d. (n=3).

In the next step, the prepared liposomes at each DOTAP:NaChol ratio were complexed with siRNA to make lipoplexes ranging from 4:1 to 16:1 (liposome:siRNA). The lipoplexes were then characterized in terms of size and surface charge (**Figure 5.2).** The results of this study showed that all lipoplexes at 4:1 (liposome:siRNA) ratios had negative surface charges with sizes ranging from 120-200 nm. This suggests that at 4:1 ratio a portion of the siRNA molecules remained unneutralized indicating that the number of positively charged liposomes in the solution was not sufficient to complex with all siRNA molecules. To test this hypothesis, we performed a gel retardation assay on

liposome-siRNA complexes. For this purpose, we chose DOTAP:NaChol liposomes at 8:1 ratio as an example and prepared liposome-siRNA complexes ranging from 1:1 to 16:1. Then, all lipoplexes were loaded onto an agarose gel followed by visualization of siRNA mobility retardation. The results of this assay confirmed our observations (**Figure 5.2)** that lipoplexes at 1:1 and 1:4 ratios were not fully condensed as evidenced by the free unbound siRNA, whereas lipoplexes at 8:1 ratio or higher could fully neutralize siRNA charges and no free siRNA was detected **(Figure 5.3)**.

Further analysis of the particle size showed that as the liposome:siRNA ratio increased from 8:1 to 16:1, the sizes of the lipoplexes decreased in all formulations and stabilized to approximately 75nm. Furthermore, in comparison to uncomplexed liposomes (**Figure 5.1)**, the surface charges of the lipoplexes at these ratios were reduced significantly from 37 mV to maximum 18 mV **(Figure 5.2)**.

Having learned that liposome-siRNA complexes at ratios higher than 4:1 are able to fully condense siRNA into small positively charged nanoparticles, we evaluated the ability of these formulations to permeate through the skin and reach the upper dermis. Since the liposome-siRNA complexes at 4:1 ratio had large sizes and negative surface charges, we used these in skin permeability studies as negative controls.

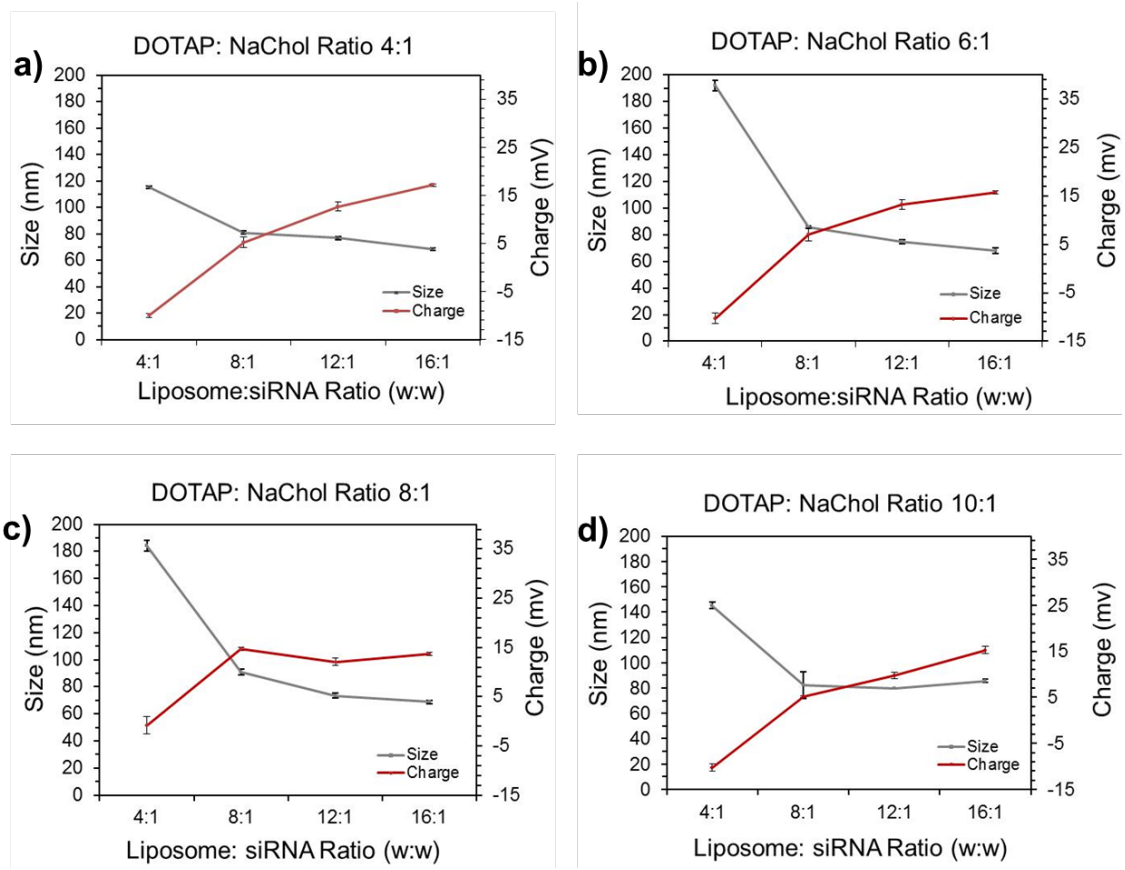

Figure 5.2: Size and zeta potential analysis of liposome-siRNA complexes at different w:w ratios ranging from 4:1 to 16:1. Data are reported as means ± s.d. (n=3).

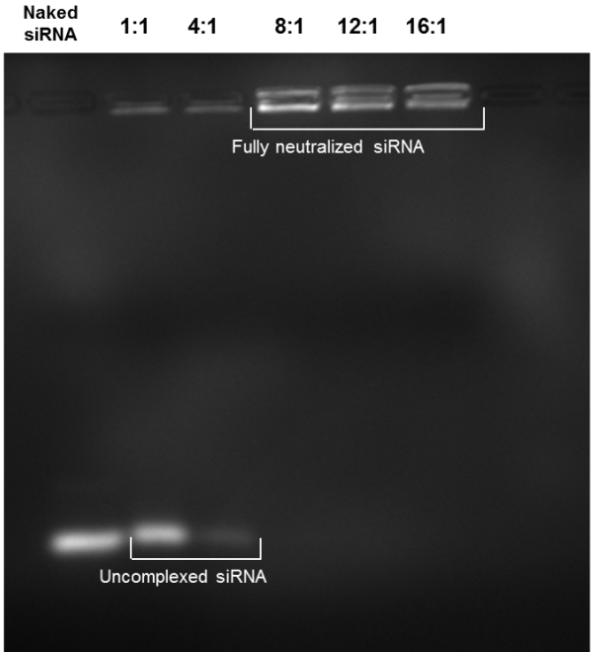

Figure 5.3: Gel retardation assay of liposome-siRNA complexes. DOTAP:NaChol (8:1) was complexed with siRNA at different ratios ranging from 1:1 to 16:1 (w:w) followed by visualization of siRNA mobility on the agarose gel. Naked siRNA was used as control.

5.2.2. Evaluation of the skin Permeability of Liposome-siRNA Complexes

To evaluate the ability of the formulated liposome-siRNA complexes (4:1 to 16:1 ratios) to diffuse through the human cadaver skin, DOTAP-NBD with green fluorescence was used to prepare the liposomes. The qualitative and quantitative analysis of results showed that DOTAP:NaChol liposomes prepared at ratio of 8:1 and in complexation with siRNA at ratios of 8:1, 12:1 and 16:1 had the highest rates of skin permeation (**Figure 5.4A and B**). Among these three formulations, liposomes prepared with DOTAP:NaChol at 8:1 ratio and complexed with siRNA at the 16:1 ratio had the highest rate of permeation through the skin layers with significant deposition at upper dermis. The analysis of green fluorescence in the skins treated with liposome-siRNA at 8:1 and 12:1

ratios showed diffusion of complexes into the lower layers of the dermis whereas lipoplexes at 16:1 ratio had significant deposition on the upper layers of dermis. Notable, that all three lipoplexes (8:1, 12:1 and 16:1 ratios) had almost identical sizes (~75 nm). Therefore, lipoplex size could not have contributed to such significant differences in skin permeation **(Figure 5.2)**. The fact that DOTAP:NaChol liposomes at 8:1 ratio penetrated through the stratum corneum and deep into the epidermis more efficiently than other groups (i.e., 4:1, 6:1 and 10:1) could be attributed to the optimum balance of the lipid (DOTAP) and edge activator (NaChol) in the liposome structure. This explanation is consistent with the observations of other groups which have reported the important role of edge activator in skin permeation of liposomes [53]. In addition to the efficient permeation through the skin layers, it was interesting to observe that as the ratio of liposome (8:1) to siRNA increased, the deposition in the upper dermis/basal epidermis increased. It has previously been demonstrated that negatively charged liposomes equipped with edge activator and sizes of less than 100 nm can permeate through the skin layers and continue their journey until they reach the micro-vessels and enter the blood stream with minimal deposition into the skin [123]. Therefore, it is logical to hypothesize that positively charged lipoplexes which can easily interact with the negative charges on the surfaces of the cell membranes are prevented from further diffusion and remain in the basal epidermis due to internalization into the cells [124, 125]. Overall, our findings highlight that particle size, surface charge, edge activator content and liposome:siRNA ratio play important roles in the effective permeation through straturm corneum/epidermis and deposition in upper dermis. These data impact the progressing in topical siRNA delivery since in the past it was thought that active delivery was necessary

to transport siRNA in therapeutically significant levels to skin layers. In our study we have shown that passive delivery (dependent on a concentration gradient) is able to achieve similar skin levels of the active [52, 114].

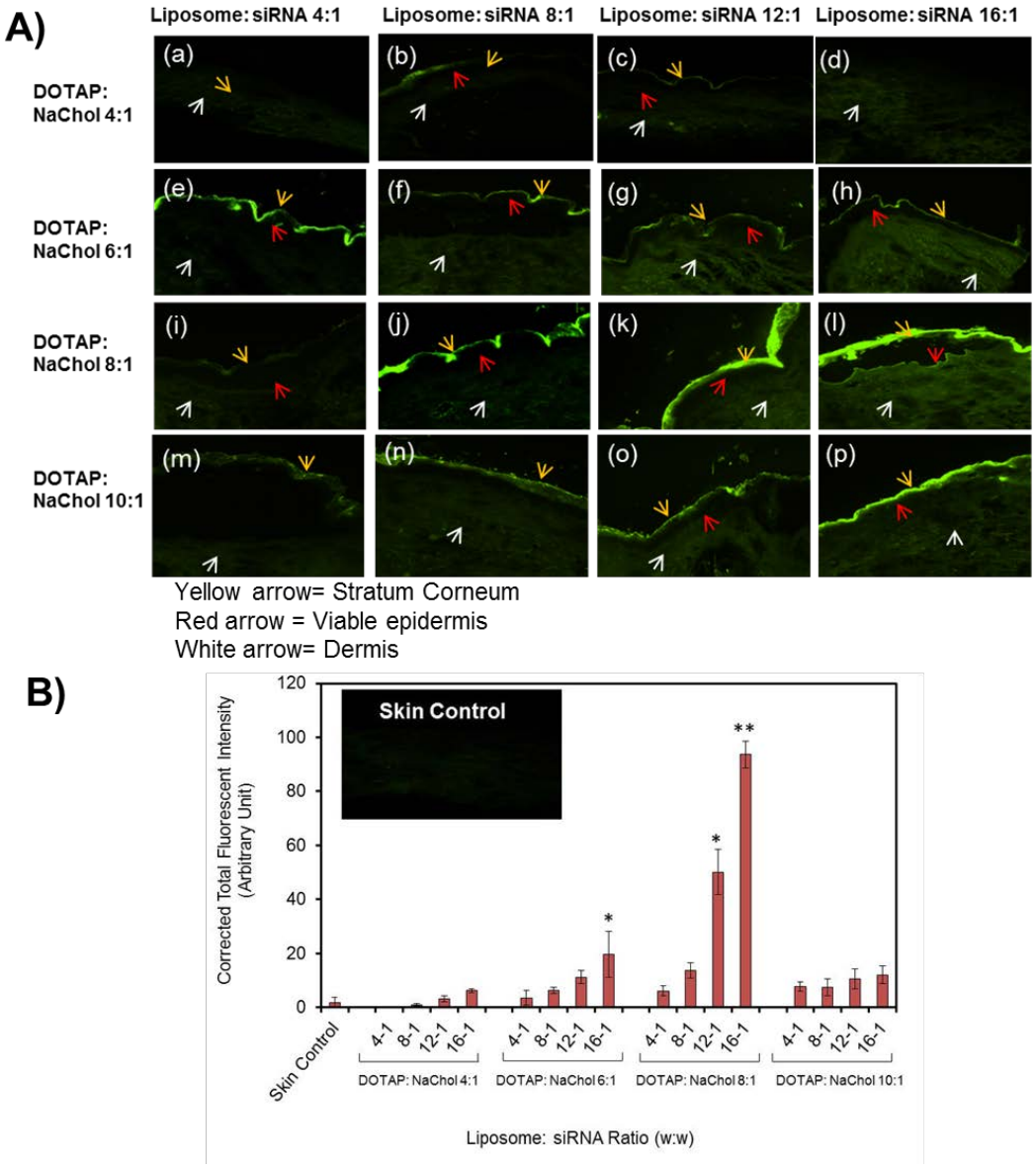

Figure 5.4: Skin permeation of liposomes-siRNA complexes. A) Fluorescent microscopy images of liposome-siRNA complexes permeated through the skin layers. a-d) Liposome (DOTAP-NBD, green fluorescence: NaChol 4:1)- siRNA complexes at w:w ratios of 4:1, 8:1, 12:1, 16:1, respectively. e-h) Liposome (DOTAP-NBD, green fluorescence: NaChol

6:1)- siRNA complexes at w:w ratios of 4:1, 8:1, 12:1, 16:1, respectively. i-l): Liposome (DOTAP-NBD, green fluorescence: NaChol 8:1) siRNA complexes at w:w ratios of 4:1, 8:1, 12:1, 16:1, respectively. m-p): Liposome (DOTAP-NBD, green fluorescence: NaChol 10:1)-siRNA complexes at w:w ratios of 4:1, 8:1, 12:1, 16:1, respectively. B) Quantification of fluorescent intensity of the deposited lipoplexes in the skin. Data are reported as means ± s.d. (n=3).

To investigate and quantify the amount of siRNA that was carried by the liposomes into each skin layer, DOTAP:NaChol liposomes (8:1) were complexed with the red fluorescently labeled siRNA (siGLO) and applied on the human cadaver skin. The analysis of data showed that lipoplexes could overcome the stratrum corneum barrier and effectively permeate the skin and deliver the siRNA mainly to the basal epidermis and upper dermis **(Figure 5.5A-C).** This observation also indicates that liposomes remained in complex with siRNA and did not dissociate. We also analyzed the media in the Franz cell receptor compartment by fluorescence spectrophotometry to see whether any labeled liposome or siRNA could be detected. The results revealed that neither liposome nor siRNA was present in the media in detectible concentrations suggesting that the lipoplexes did not cross the dermis to reach the receptor compartment. This is an important observation since it points at more localized therapeutic effects and less probability of observing systemic toxicity after administration.

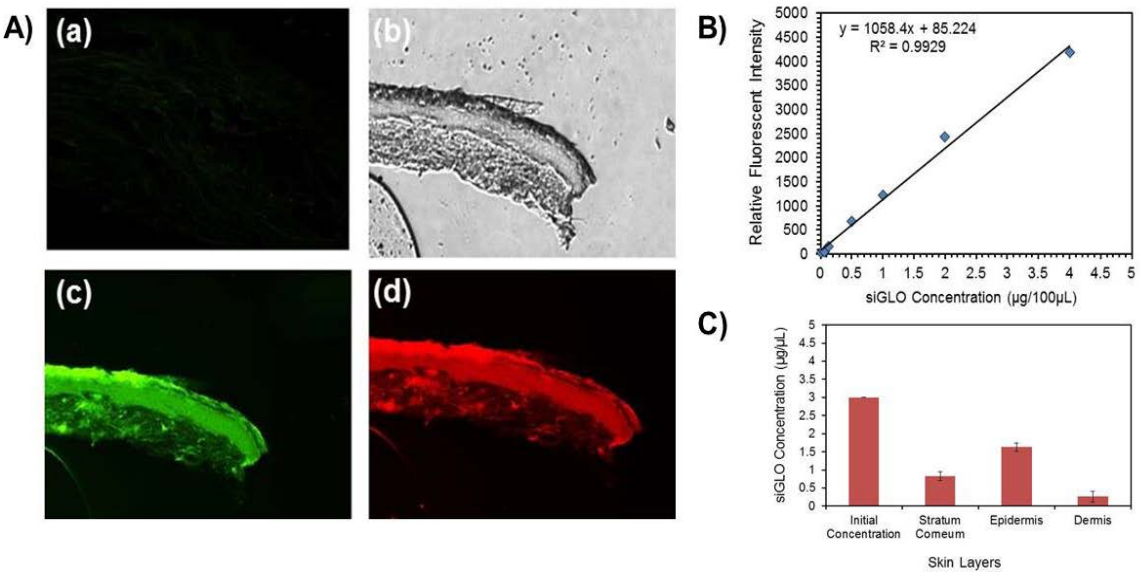

Figure 5.5: Skin permeation of lipoplexes ratio 16:1 (w:w). A) Representative fluorescent microscope images of lipoplexes prepared through complexation of liposomes (DOTAP-NBD, green fluorescence: NaChol ratio 8:1 (w:w) and siRNA (siGLO, red fluorescence) (16:1 w:w) and delivery of siRNA into deep layers of the skin. (a) Skin control. (b) Phase image of the skin that shows each skin layer. (c) Liposomes. (d) Liposome-siRNA complexes. B) Calibration curve used for the quantification of siRNA in each skin layer. C) Quantification of siRNA in each skin layer based on the red fluorescence intensity of each layer. The initial concentration of siRNA was 3µg. Data are reported as means ± s.d. (n=3).

5.2.3. Intracellular Localization of the Lipoplexes and Protein Expression Knockdown

In the next part of the study we examined the ability of lipoplexes to internalize into human melanoma cells as they are the ultimate target for the developed siRNA delivery system. For this purpose, green fluorescent labeled DOTAP:Nachol (8:1) liposomes were

complexed with siGLO at 16:1 ratio and used to transfect UACC-903 melanoma cells. This particular formulation of lipoplexes was chosen based on the previous experiments that showed the highest rate of permeation through the skin layers. The results of this study showed that the lipoplexes could effectively internalize and localize into the cytoplasm of melanoma cells **(Figure 5.6)**; thereby, raising the possibility of effective protein expression knockdown in these cells. To examine whether the lipoplexes could release the siRNA inside the cytoplasm which in turn would result in protein expression knockdown, we performed the next set of studies using therapeutic BRAF siRNA.

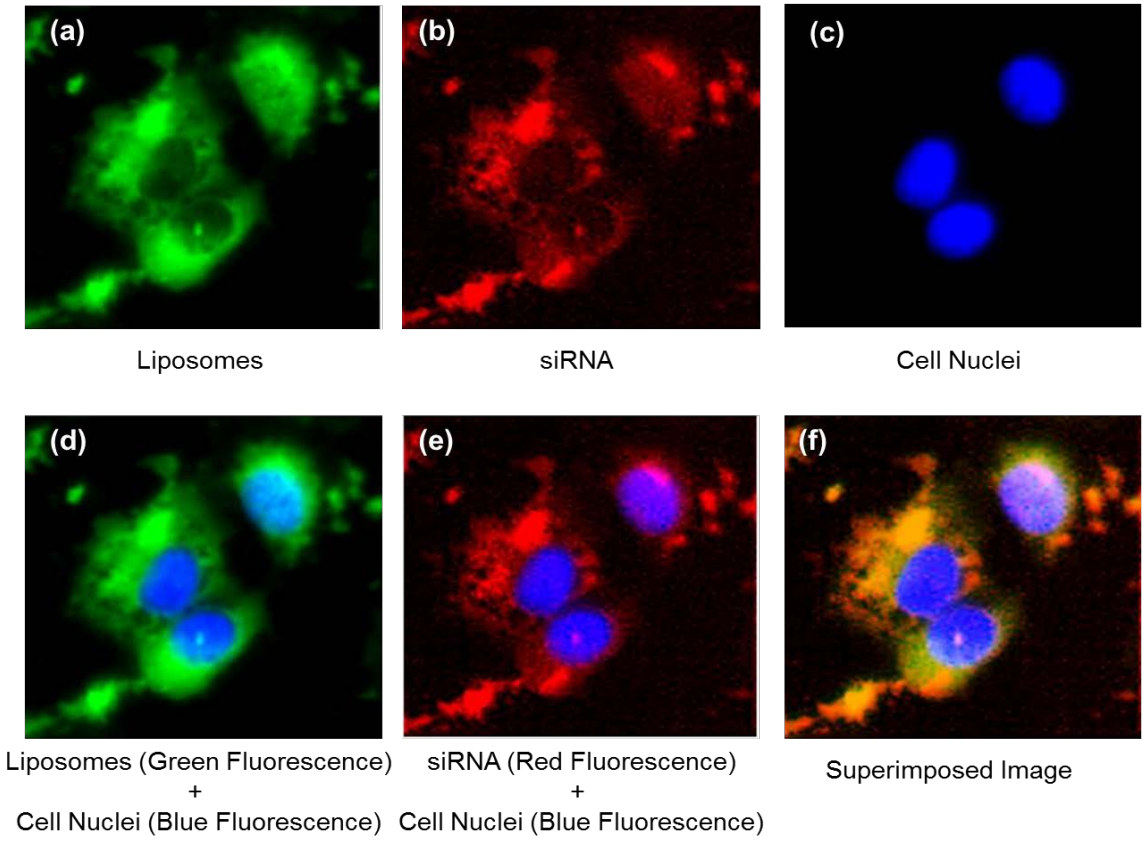

Figure 5.6: Intracellular localization of liposomes and siRNA. Typical images of human UACC 903 melanoma cells incubated for 1 hour with liposomes (DOTAP-NBD, green fluorescence) in complex with siRNA (siGLO, red fluorescence). Cell nuclei were stained

with nuclear-specific dye DAPI (blue fluorescence). Superimposed image shows co-localization of liposomes and siRNA.

5.2.4. Evaluation of BRAF Expression Knockdown by Lipoplexes

In the next step, we evaluated the ability of the liposomes in complex with BRAF *(V600E)* siRNA to knockdown the protein expression. BRAF is a serine/threonine kinase protein involved in the MAPK/ERK signaling pathway and upon activation, it signals for the cell process regulation such as gene expression, cell proliferation, differentiation, and apoptosis [126]. In the case of an oncogenic gene mutation in the MAPK pathway, cells grow and differentiate aggressively and develop tumors. As was mentioned previously, 60% of melanoma cases are caused by a point mutation in the gene that encodes BRAF protein and 90% of these mutations involve substitution of valine for glutamic acid at the 600 amino acid of the protein (V600E). Therefore, by delivering siRNA targeted to the mutated *BRAF* RNA, the expression of the BRAF protein can be attenuated which can consequently reduce melanoma cells proliferation.

Using *BRAF (V600E)* siRNA, lipoplexes at 16:1 ratio were prepared as mentioned above and used to transfect UACC-903 melanoma cells. This combination of siRNA and melanoma cell line was chosen since the selective silencing effect of the *BRAF (V600E)* siRNA on UACC-903 and other human melanoma cells has been reported in the literature [127-130]. The BRAF protein expression levels inside the treated cells were measured by using in-cell immunofluorescence assay **(Figure 5.7**). The results of this study did not reveal BRAF protein expression knockdown in cells that were treated with

empty liposomes, naked BRAF siRNA or liposomes in complex with scrambled siRNA (control groups). In contrast, the BRAF protein expression level was significantly reduced in cells that were treated with liposomes in complex with BRAF siRNA. This indicates that the lipoplex formulation could internalize, release the therapeutic siRNA into the cytoplasm of melanoma cells and effectively down regulate the expression of the BRAF protein.

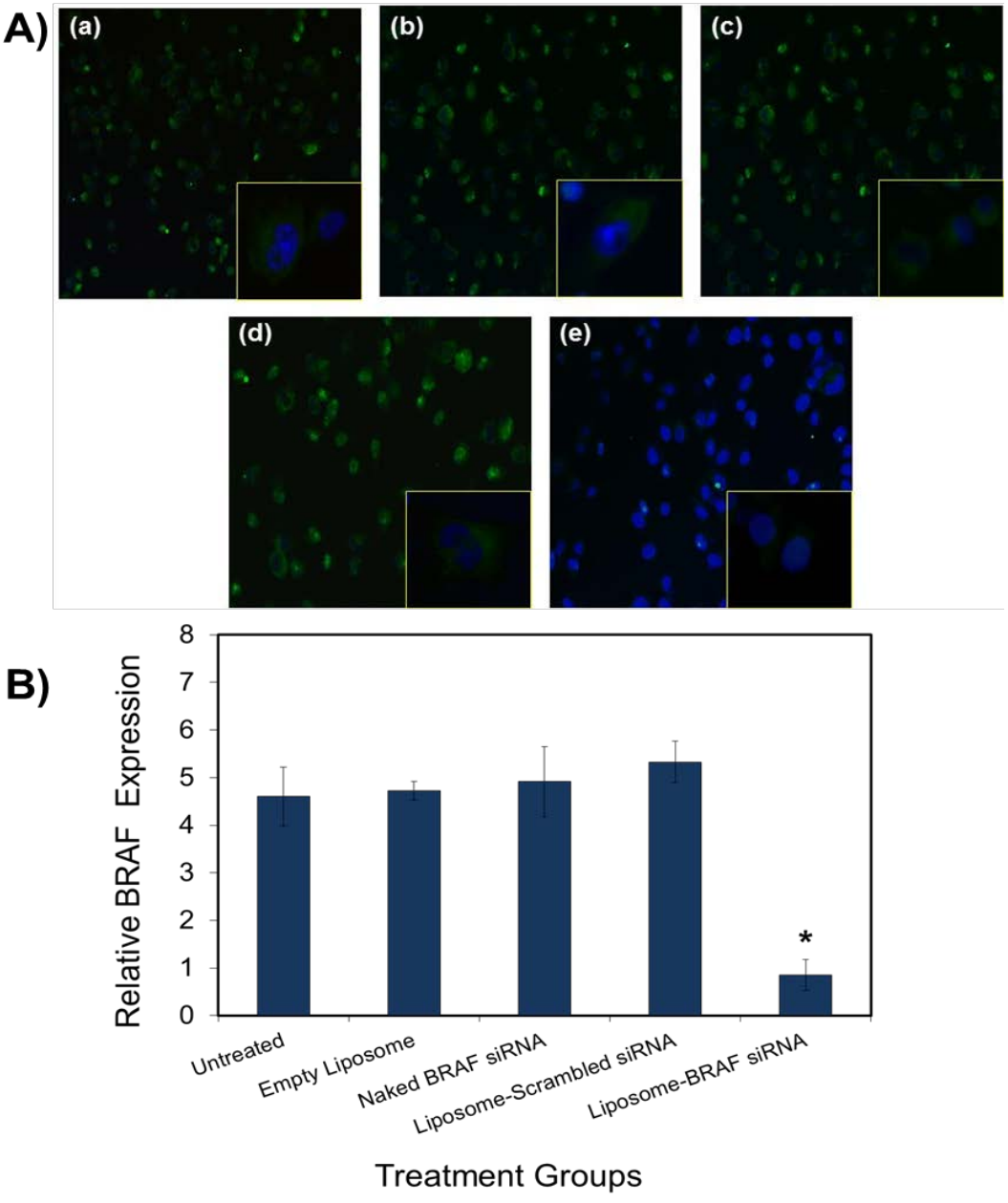

Figure 5.7: In-cell Immunofluorescence assay of UACC-903 melanoma cells treated with lipsome/BRAF-siRNA.A) Qualitative analysis of BRAF protein expression knockdown in cells: (a) untreated; (b) treated with empty liposomes; (c) treated with naked BRAF siRNA; (d) treated with liposome containing scrambled siRNA; and (e) treated with liposome-BRAF siRNA complexes. B) Quantitative analysis of protein expression knockdown. Data are reported as mean ± s.d. (n=3).

We further examined the ability of the formulated lipoplexes carrying BRAF siRNA to inhibit the proliferation of melanoma cells. Therefore, lipoplexes were prepared at 16:1 ratio using BRAF-siRNA (ranging from 0.1 to 0.5 μg) and then used to transfect UACC-903 melanoma cells. The impact of the prepared lipoplexes on melanoma cell proliferation was evaluated by using WST-1 cell proliferation assay. UACC-903 human melanoma cell line was used as a model because it has been reported that this cell line contains high levels of mutated *BRAF* V600E [129, 131]. The results of this study showed that lipolexes carrying at least 0.5 μg of BRAF siRNA were able to significantly reduce the viability of the melanoma cells **(Figure 5.8)**. In contrast, liposomes carrying 0.5 μg of the scrambled siRNA did not induce any toxic effects on melanoma cells.

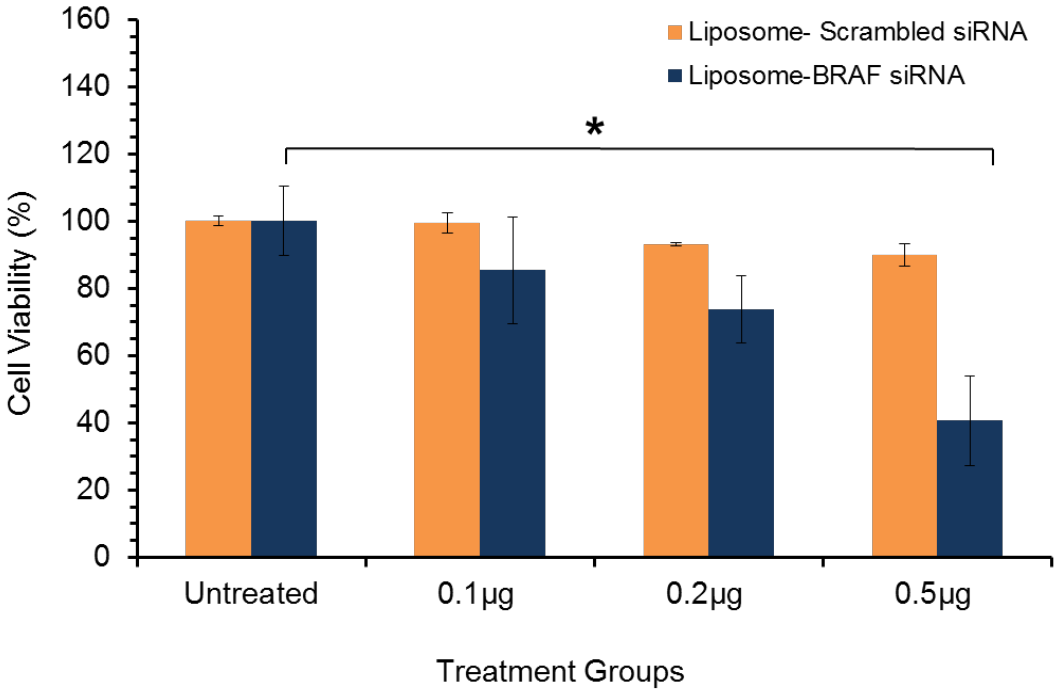

Figure 5.8: WST-1 cell proliferation assay. Evaluation of toxicity in UACC-903 human melanoma cells treated with liposome-*BRAF* siRNA complexes (Equivalent of 0.1, 0.2 and 0.5µg siRNA). Liposome-Scrambled siRNA complexes at the same concentrations were used as controls. Data are reported as mean ± s.d. (n=3).

5.2.5. Rheological Measurement and In vitro Release Study

In the next part of our study, we formulated topical gels from the prepared lipoplexes. Two concentrations of gel (0.5% and 1%) were prepared using Carbopol 934 and then the lipoplexes were incorporated in them mechanically. As a vehicle for incorporation of the lipoplexes, we selected carbopol 934 due to its compatibility with liposomes [121, 132]. Carbopol is a synthetic carboxyvinyl polymer that are commonly used for topical gels within concentrations from 0.5% to 2% [133]. Carbopol gels are uniform, more stable and resistant to microbial and fungal growth due to their good viscosity even in low

concentrations. The final gels, loaded or not loaded with lipoplexes were examined for their rheological properties. For each gel, storage (G´) and loss moduli (G″) were measured over a frequency range of 100-1 rad/s. The lipoplex concentration incorporated in each gel was 10% (w:w). **Figure 5.9** shows rheological curves of 0.5% and 1% gel each before and after addition of the lipoplexes. The curves for all the gels show that the curves were almost frequency dependent and G´ moduli (elastic response) were at least 10 times higher than G″ moduli (viscous behavior) suggesting the formation of an elastic gel with being more elastic for the 1% gel [134, 135]. Moreover, our results suggest that the liposomes were compatible with the gel and their presence did not influence the gelation properties. Our results are consistent with other liposomal gel formulations [122, 136].

In the next step, we investigated the release profile of lipoplexes from each gel formulation. The release of lipoplexes was monitored by collecting the receptor at each predetermined time point using a fluorescence spectrophotometer. The cumulative amount released of the lipoplexes was then correlated to the fluorescent intensity of the lipoplexes using a standard curve. The cumulative release (%) of lipoplexes from each gel is shown in **Figure 5.10.** The results suggest that the release of lipoplexes from gel 0.5% was relatively faster and could release more than 80% of the lipoplexes over 72hours. On the other hand, the release of lipoplex formulation was very slow from 1% gel and most of the formulation was retained by the gel. These findings are consistent with the viscoelastic properties of the gels that the 0.5% formulation is more viscous than the 1%.

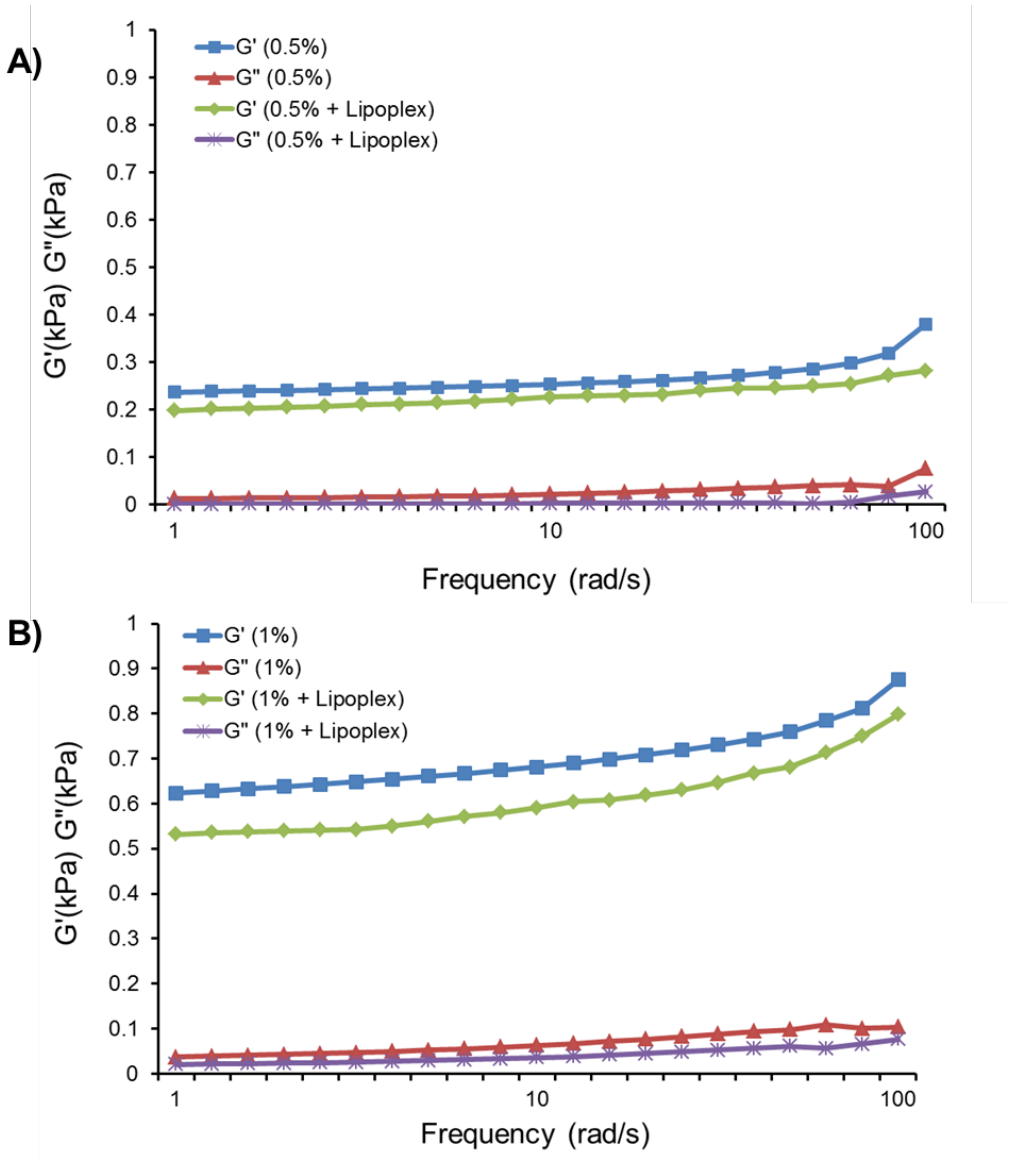

Figure 5.9: Rheological measurement of carbopol gels. A) Storage moduli (G´) and loss moludi (G″) of gel 1% before and after adding the lipoplex formulation. B) Storage moduli (G´) and loss moduli(G″) of gel 0.5% before and after adding the lipoplex formulation.

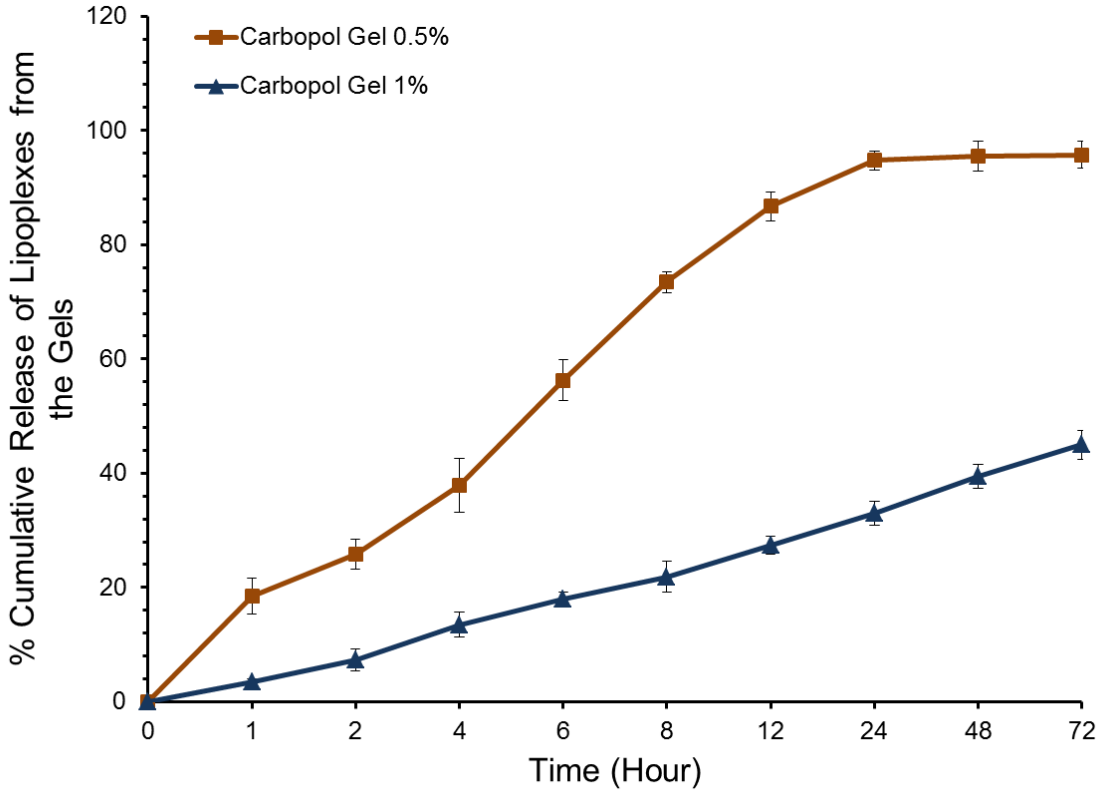

Figure 5.10: Percent cumulative release of the fluorescently labeled lipoplexes from carbopol gel 0.5% and 1%.

5.2.6. In vitro Skin Permeation

Having learned that the 0.5% carbopol gel can release the lipoplexes in a timely manner, we examined its skin permeation for 8 and 24 hours using Franz diffusion techniques. **Figure 5.11** represents permeation of lipoplexes into human cadaver skin at these two different time points. After 24 hours, the lipoplexes could go all through the dermis (**5.11b and c**). We should also note that in the media analysis of the Franz cells using fluorescence spectrophotometry we could detect some traces of the lipoplexes in the receptor. In an attempt to observe if we had restricted skin deposition of the lipoplexes in the epidermis we collected the skin samples after 8 hours. The data suggest that the intact

lipoplexes successfully permeated through the stratum corneum and deep into the viable epidermis (**Figure 5.11 e and f**). The analysis of the receptor fluid did not show any traces of the lipoplexes suggesting that the formulation was retained in the epidermis.

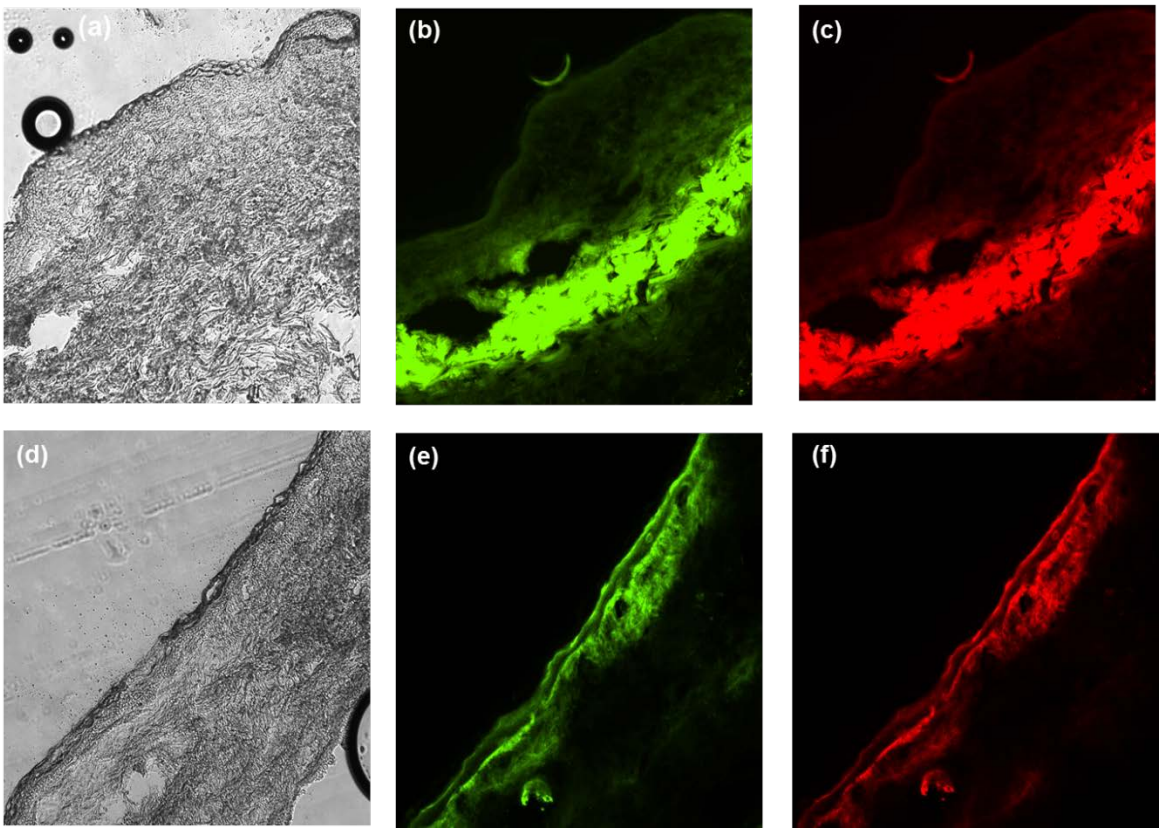

Figure 5.11: Skin permeation of lipoplexes incorporated in carbopol gel 0.5%. (a)-(c): After 24h (d)-(f) after 8h. (a) Phase image of the skin that shows each skin layer. (b) Liposomes. (c) Liposome-siRNA complex. (d) Phase image of the skin showing each skin layer. (b) Liposomes. (f) Liposome-siRNA complex.

5.3. Conclusion

The results of this study demonstrate that for the efficient siRNA delivery through the skin layers (i.e., stratum corneum and epidermis) and deposition in the upper dermis a correct balance of lipoplex size, charge and edge activator content is required. The

developed lipoplexes were able to not only permeate through the skin layers but also effectively internalize into the viable cells of basal epidermis and knockdown the expression of target proteins. Given that no active delivery approach such as ultrasound was used to enhance skin permeation, the developed liposomal system can be considered a major step forward towards a simple and efficient drug delivery of macromolecules via the topical route for therapy of various skin diseases. In addition, incorporation of liposome-siRNA complexes in a compatible gel can improve the skin permeation and deposition of lipoplexes in a shorter time and with a lower dose.

References

[1] E. Fattal, A. Bochot, State of the art and perspectives for the delivery of antisense oligonucleotides and siRNA by polymeric nanocarriers, Int J Pharm, 364 (2008) 237-248.

[2] C.L. Simpson, D.M. Patel, K.J. Green, Deconstructing the skin: cytoarchitectural determinants of epidermal morphogenesis, Nat Rev Mol Cell Biol, 12 (2011) 565-580.

[3] I.H. Blank, Further observations on factors which influence the water content of the stratum corneum, J Invest Dermatol, 21 (1953) 259-271.

[4] T. Windsor, G.E. Burch, Rate of insensible perspiration (diffusion of water) locally through living and through dead human skin, Arch Intern Med, 74 (1944) 428-444.

[5] M. Forster, M.A. Bolzinger, H. Fessi, S. Briancon, Topical delivery of cosmetics and drugs. Molecular aspects of percutaneous absorption and delivery, Eur J Dermatol, 19 (2009) 309-323.

[6] S.N. Andrews, E. Jeong, M.R. Prausnitz, Transdermal delivery of molecules is limited by full epidermis, not just stratum corneum, Pharm Res, 30 (2013) 1099-1109.

[7] K. Morita, Y. Miyachi, M. Furuse, Tight junctions in epidermis: from barrier to keratinization, Eur J Dermatol, 21 (2011) 12-17.

[8] S. Jang, M.B. Atkins, Treatment of BRAF-mutant melanoma: the role of vemurafenib and other therapies, Clin Pharmacol Ther, 95 (2014) 24-31.

[9] L. Santarpia, S.M. Lippman, A.K. El-Naggar, Targeting the MAPK-RAS-RAF signaling pathway in cancer therapy, Expert Opin Ther Targets, 16 (2012) 103-119.

[10] T. Huang, J. Zhuge, W.W. Zhang, Sensitive detection of BRAF V600E mutation by Amplification Refractory Mutation System (ARMS)-PCR, Biomark Res, 1 (2013) 3.

[11] G.V. Long, A.M. Menzies, A.M. Nagrial, L.E. Haydu, A.L. Hamilton, G.J. Mann, T.M. Hughes, J.F. Thompson, R.A. Scolyer, R.F. Kefford, Prognostic and clinicopathologic associations of oncogenic BRAF in metastatic melanoma, J Clin Oncol, 29 (2011) 1239-1246.

[12] A. Fire, S. Xu, M.K. Montgomery, S.A. Kostas, S.E. Driver, C.C. Mello, Potent and specific genetic interference by double-stranded RNA in Caenorhabditis elegans, Nature, 391 (1998) 806-811.

[13] S. Liang, A. Sharma, H.H. Peng, G. Robertson, C. Dong, Targeting mutant (V600E) B-Raf in melanoma interrupts immunoediting of leukocyte functions and melanoma extravasation, Cancer Res, 67 (2007) 5814-5820.

[14] M.A. Tran, R. Gowda, A. Sharma, E.J. Park, J. Adair, M. Kester, N.B. Smith, G.P. Robertson, Targeting V600EB-Raf and Akt3 using nanoliposomal-small interfering RNA inhibits cutaneous melanocytic lesion development, Cancer Res, 68 (2008) 7638-7649.

[15] Y. Itoh, A. Shimazu, Y. Sadzuka, T. Sonobe, S. Itai, Novel method for stratum corneum pore size determination using positron annihilation lifetime spectroscopy, Int J Pharm, 358 (2008) 91-95.

[16] S.F. Ng, J.J. Rouse, F.D. Sanderson, G.M. Eccleston, The relevance of polymeric synthetic membranes in topical formulation assessment and drug diffusion study, Arch Pharm Res, 35 (2012) 579-593.

[17] J. Martinez, A. Patkaniowska, H. Urlaub, R. Luhrmann, T. Tuschl, Single-stranded antisense siRNAs guide target RNA cleavage in RNAi, Cell, 110 (2002) 563-574.

[18] D. Castanotto, J.J. Rossi, The promises and pitfalls of RNA-interference-based therapeutics, Nature, 457 (2009) 426-433.

[19] B.L. Davidson, P.B. McCray, Jr., Current prospects for RNA interference-based therapies, Nat Rev Genet, 12 (2011) 329-340.

[20] R. Kanasty, J.R. Dorkin, A. Vegas, D. Anderson, Delivery materials for siRNA therapeutics, Nat Mater, 12 (2013) 967-977.

[21] D. Zheng, D.A. Giljohann, D.L. Chen, M.D. Massich, X.Q. Wang, H. Iordanov, C.A. Mirkin, A.S. Paller, Topical delivery of siRNA-based spherical nucleic acid nanoparticle conjugates for gene regulation, Proc Natl Acad Sci U S A, 109 (2012) 11975-11980.

[22] J. Wang, Z. Lu, M.G. Wientjes, J.L. Au, Delivery of siRNA therapeutics: barriers and carriers, AAPS J, 12 (2010) 492-503.

[23] C. Foged, siRNA delivery with lipid-based systems: promises and pitfalls, Curr Top Med Chem, 12 (2012) 97-107.

[24] S.A. Leachman, R.P. Hickerson, M.E. Schwartz, E.E. Bullough, S.L. Hutcherson, K.M. Boucher, C.D. Hansen, M.J. Eliason, G.S. Srivatsa, D.J. Kornbrust, F.J. Smith, W.I. McLean, L.M. Milstone, R.L. Kaspar, First-in-human mutation-targeted siRNA phase Ib trial of an inherited skin disorder, Mol Ther, 18 (2010) 442-446.

[25] R.F. Donnelly, T.R. Raj Singh, A.D. Woolfson, Microneedle-based drug delivery systems: microfabrication, drug delivery, and safety, Drug Deliv, 17 (2010) 187-207.

[26] J. Birchall, S. Coulman, A. Anstey, C. Gateley, H. Sweetland, A. Gershonowitz, L. Neville, G. Levin, Cutaneous gene expression of plasmid DNA in excised human skin following delivery via microchannels created by radio frequency ablation, Int J Pharm, 312 (2006) 15-23.

[27] S.A. Coulman, D. Barrow, A. Anstey, C. Gateley, A. Morrissey, N. Wilke, C. Allender, K. Brain, J.C. Birchall, Minimally invasive cutaneous delivery of macromolecules and plasmid DNA via microneedles, Curr Drug Deliv, 3 (2006) 65-75.

[28] J.A. Mikszta, V.J. Sullivan, C. Dean, A.M. Waterston, J.B. Alarcon, J.P. Dekker, 3rd, J.M. Brittingham, J. Huang, C.R. Hwang, M. Ferriter, G. Jiang, K. Mar, K.U. Saikh, B.G. Stiles, C.J. Roy, R.G. Ulrich, N.G. Harvey, Protective immunization against inhalational anthrax: a comparison of minimally invasive delivery platforms, J Infect Dis, 191 (2005) 278-288.

[29] R.K. Sivamani, D. Liepmann, H.I. Maibach, Microneedles and transdermal applications, Expert Opin Drug Deliv, 4 (2007) 19-25.

[30] E. Gonzalez-Gonzalez, T.J. Speaker, R.P. Hickerson, R. Spitler, M.A. Flores, D. Leake, C.H. Contag, R.L. Kaspar, Silencing of reporter gene expression in skin using siRNAs and expression of plasmid DNA delivered by a soluble protrusion array device (PAD), Mol Ther, 18 (2010) 1667-1674.

[31] R.H. Chong, E. Gonzalez-Gonzalez, M.F. Lara, T.J. Speaker, C.H. Contag, R.L. Kaspar, S.A. Coulman, R. Hargest, J.C. Birchall, Gene silencing following siRNA delivery to skin via coated steel microneedles: In vitro and in vivo proof-of-concept, J Control Release, 166 (2013) 211-219.

[32] M. Dorrani, M. Kaul, A. Parhi, E.J. LaVoie, D.S. Pilch, B. Michniak-Kohn, TXA497 as a topical antibacterial agent: Comparative antistaphylococcal, skin deposition, and skin permeation studies with mupirocin, Int J Pharm, 476 (2014) 199-204.

[33] T. Uchida, T. Kanazawa, Y. Takashima, H. Okada, Development of an efficient transdermal delivery system of small interfering RNA using functional peptides, Tat and AT-1002, Chem Pharm Bull (Tokyo), 59 (2011) 196-201.

[34] T. Hsu, S. Mitragotri, Delivery of siRNA and other macromolecules into skin and cells using a peptide enhancer, Proc Natl Acad Sci U S A, 108 (2011) 15816-15821.

[35] S. Kumar, M. Zakrewsky, M. Chen, S. Menegatti, J.A. Muraski, S. Mitragotri, Peptides as skin penetration enhancers: Mechanisms of action, J Control Release, 199 (2015) 168-178.

[36] A.K. Varkouhi, S. Foillard, T. Lammers, R.M. Schiffelers, E. Doris, W.E. Hennink, G. Storm, SiRNA delivery with functionalized carbon nanotubes, Int J Pharm, 416 (2011) 419-425.

[37] S. Foillard, G. Zuber, E. Doris, Polyethylenimine-carbon nanotube nanohybrids for siRNA-mediated gene silencing at cellular level, Nanoscale, 3 (2011) 1461-1464.

[38] N.W. Kam, Z. Liu, H. Dai, Functionalization of carbon nanotubes via cleavable disulfide bonds for efficient intracellular delivery of siRNA and potent gene silencing, J Am Chem Soc, 127 (2005) 12492-12493.

[39] A. Kichler, C. Leborgne, E. Coeytaux, O. Danos, Polyethylenimine-mediated gene delivery: a mechanistic study, J Gene Med, 3 (2001) 135-144.

[40] J. Wu, K.S. Paudel, C. Strasinger, D. Hammell, A.L. Stinchcomb, B.J. Hinds, Programmable transdermal drug delivery of nicotine using carbon nanotube membranes, Proc Natl Acad Sci U S A, 107 (2010) 11698-11702.

[41] K.S. Siu, D. Chen, X. Zheng, X. Zhang, N. Johnston, Y. Liu, K. Yuan, J. Koropatnick, E.R. Gillies, W.P. Min, Non-covalently functionalized single-walled carbon nanotube for topical siRNA delivery into melanoma, Biomaterials, 35 (2014) 3435-3442.

[42] V. Shah, O. Taratula, O.B. Garbuzenko, M.L. Patil, R. Savla, M. Zhang, T. Minko, Genotoxicity of different nanocarriers: possible modifications for the delivery of nucleic acids, Curr Drug Discov Technol, 10 (2013) 8-15.

[43] D. Libster, A. Aserin, N. Garti, Interactions of biomacromolecules with reverse hexagonal liquid crystals: drug delivery and crystallization applications, J Colloid Interface Sci, 356 (2011) 375-386.

[44] F.T. Vicentini, L.V. Depieri, A.C. Polizello, J.O. Del Ciampo, A.C. Spadaro, M.C. Fantini, M. Vitoria Lopes Badra Bentley, Liquid crystalline phase nanodispersions enable skin delivery of siRNA, Eur J Pharm Biopharm, 83 (2013) 16-24.

[45] M. Mezei, V. Gulasekharam, Liposomes--a selective drug delivery system for the topical route of administration. Lotion dosage form, Life Sci, 26 (1980) 1473-1477.

[46] R. Gupta, M. Gupta, S. Mangal, U. Agrawal, S.P. Vyas, Capsaicin-loaded vesicular systems designed for enhancing localized delivery for psoriasis therapy, Artif Cells Nanomed Biotechnol, (2014) 1-10.

[47] M.I. Nounou, L.K. El-Khordagui, N.A. Khalafallah, S.A. Khalil, Liposomal formulation for dermal and transdermal drug delivery: past, present and future, Recent Pat Drug Deliv Formul, 2 (2008) 9-18.

[48] N. Sun, Y. Zhu, L. Yuan, B. Lang, Nano-liposomes of entrapment lidocaine hydrochloride on in vitro permeability of narcotic, Pak J Pharm Sci, 28 (2015) 325-328.

[49] J. Pardeike, A. Hommoss, R.H. Muller, Lipid nanoparticles (SLN, NLC) in cosmetic and pharmaceutical dermal products, Int J Pharm, 366 (2009) 170-184.

[50] G. Cevc, G. Blume, Lipid vesicles penetrate into intact skin owing to the transdermal osmotic gradients and hydration force, Biochim Biophys Acta, 1104 (1992) 226-232.

[51] S. Goindi, G. Kumar, A. Kaur, Novel flexible vesicles based topical formulation of levocetirizine: in vivo evaluation using oxazolone-induced atopic dermatitis in murine model, J Liposome Res, 24 (2014) 249-257.

[52] B. Geusens, J. Lambert, S.C. De Smedt, K. Buyens, N.N. Sanders, M. Van Gele, Ultradeformable cationic liposomes for delivery of small interfering RNA (siRNA) into human primary melanocytes, J Control Release, 133 (2009) 214-220.

[53] B. Geusens, M. Van Gele , S. Braat , S.C. De Smedt , M.C.A. Stuart , T.W. Prow , W. Sanchez , M.S. Roberts , N.N. Sanders , J. Lambert, Flexible Nanosomes (SECosomes) Enable Efficient siRNA Delivery in Cultured Primary Skin Cells and in the Viable Epidermis of Ex Vivo Human Skin, Adv Funct Mater, 20 (2010) 4077-4090.

[54] P.R. Desai, S. Marepally, A.R. Patel, C. Voshavar, A. Chaudhuri, M. Singh, Topical delivery of anti-TNFalpha siRNA and capsaicin via novel lipid-polymer hybrid nanoparticles efficiently inhibits skin inflammation in vivo, J Control Release, 170 (2013) 51-63.

[55] M. Chen, M. Zakrewsky, V. Gupta, A.C. Anselmo, D.H. Slee, J.A. Muraski, S. Mitragotri, Topical delivery of siRNA into skin using SPACE-peptide carriers, J Control Release, 179 (2014) 33-41.

[56] S.S. Kwon, S.Y. Kim, B.J. Kong, K.J. Kim, G.Y. Noh, N.R. Im, J.W. Lim, J.H. Ha, J. Kim, S.N. Park, Cell penetrating peptide conjugated liposomes as transdermal delivery system of Polygonumaviculare L. extract, Int J Pharm, 483 (2015) 26-37.

[57] T.J. Franz, Percutaneous absorption on the relevance of in vitro data, J Invest Dermatol, 64 (1975) 190-195.

[58] A.M. Barbero, H.F. Frasch, Pig and guinea pig skin as surrogates for human in vitro penetration studies: a quantitative review, Toxicol In Vitro, 23 (2009) 1-13.

[59] G.M. El Maghraby, B.W. Barry, A.C. Williams, Liposomes and skin: from drug delivery to model membranes, Eur J Pharm Sci, 34 (2008) 203-222.

[60] M.H. Qvist, U. Hoeck, B. Kreilgaard, F. Madsen, S. Frokjaer, Evaluation of Gottingen minipig skin for transdermal in vitro permeation studies, Eur J Pharm Sci, 11 (2000) 59-68.

[61] B.W. Barry, Modern methods of promoting drug absorption through the skin, Mol Aspects Med, 12 (1991) 195-241.

[62] B.W. Barry, A.R. Brace, Permeation of oestrone, oestradiol, oestriol and dexamethasone across cellulose acetate membrane, J Pharm Pharmacol, 29 (1977) 397-400.

[63] S.C. Chattaraj, S.K. Das, I. Kanfer, In vitro release of acyclovir from semisolid dosage forms: effect of cyclodextrin and polyethylene glycol, Pharm Dev Technol, 3 (1998) 565-570.

[64] L. Montenegro, C. Carbone, G. Condorelli, R. Drago, G. Puglisi, Effect of oil phase lipophilicity on in vitro drug release from o/w microemulsions with low surfactant content, Drug Dev Ind Pharm, 32 (2006) 539-548.

[65] V.P. Shah, J. Elkins, J. Hanus, C. Noorizadeh, J.P. Skelly, In vitro release of hydrocortisone from topical preparations and automated procedure, Pharm Res, 8 (1991) 55-59.

[66] M.P. Short, C.T. Rhodes, Some studies of the diffusion of steroids across a cellulose acetate membrane, Kolloid-Zeitschrift und Zeitschrift für Polymere, 250 (1972) 602-604.

[67] S.F. Ng, J. Rouse, D. Sanderson, G. Eccleston, A Comparative Study of Transmembrane Diffusion and Permeation of Ibuprofen across Synthetic Membranes Using Franz Diffusion Cells, Pharmaceutics, 2 (2010) 209-223.

[68] P. Santos, A.C. Watkinson, J. Hadgraft, M.E. Lane, Formulation issues associated with transdermal fentanyl delivery, Int J Pharm, 416 (2011) 155-159.

[69] V. Joshi, D. Brewster, P. Colonero, Transdermal diffusion. In vitro diffusion studies in transdermal research: a synthetic membrane model in place of human skin, Drug Dev. Delivery, 12 (2012) 40–42.

[70] G. Ottaviani, S. Martel, P.A. Carrupt, Parallel artificial membrane permeability assay: a new membrane for the fast prediction of passive human skin permeability, J Med Chem, 49 (2006) 3948-3954.

[71] D. Karadzovska, J.E. Riviere, Assessing vehicle effects on skin absorption using artificial membrane assays, Eur J Pharm Sci, 50 (2013) 569-576.

[72] M.J. Kim, H.J. Doh, M.K. Choi, S.J. Chung, C.K. Shim, D.D. Kim, J.S. Kim, C.S. Yong, H.G. Choi, Skin permeation enhancement of diclofenac by fatty acids, Drug Deliv, 15 (2008) 373-379.

[73] W. Zhu, A. Yu, W. Wang, R. Dong, J. Wu, G. Zhai, Formulation design of microemulsion for dermal delivery of penciclovir, Int J Pharm, 360 (2008) 184-190.

[74] S.G. Machatha, S.H. Yalkowsky, Estimation of the ethanol/water solubility profile from the octanol/water partition coefficient, Int J Pharm, 286 (2004) 111-115.

[75] S.G. Summerfield, A.J. Stevens, L. Cutler, M. del Carmen Osuna, B. Hammond, S.P. Tang, A. Hersey, D.J. Spalding, P. Jeffrey, Improving the in vitro prediction of in vivo central nervous system penetration: integrating permeability, P-glycoprotein efflux, and free fractions in blood and brain, J Pharmacol Exp Ther, 316 (2006) 1282-1290.

[76] B.W. Barry, D. Southwell, R. Woodford, Optimization of bioavailability of topical steroids: penetration enhancers under occlusion, J Invest Dermatol, 82 (1984) 49-52.

[77] M. Nino, G. Calabro, P. Santoianni, Topical delivery of active principles: the field of dermatological research, Dermatol Online J, 16 (2010) 4.

[78] B.W. Barry, Novel mechanisms and devices to enable successful transdermal drug delivery, Eur J Pharm Sci, 14 (2001) 101-114.

[79] J.A. Bouwstra, M. Ponec, The skin barrier in healthy and diseased state, Biochim Biophys Acta, 1758 (2006) 2080-2095.

[80] F. Cilurzo, G. Vistoli, F. Selmin, C.G. Gennari, U.M. Musazzi, S. Franze, M. Lo Monte, P. Minghetti, An insight into the skin penetration enhancement mechanism of N-methylpyrrolidone, Mol Pharm, 11 (2014) 1014-1021.

[81] T. Uchida, W.R. Kadhum, S. Kanai, H. Todo, T. Oshizaka, K. Sugibayashi, Prediction of skin permeation by chemical compounds using the artificial membrane, Strat-M, Eur J Pharm Sci, 67 (2015) 113-118.

[82] N.S. Janani, G.B. Kumar, P.B. Balakrishna, D. Sruthi, M.S. Kumar, S. Mantry, A Review on Strat-M Membrane, International Journal of Innovative Pharmaceutical Sciences, 2 (2014) 962-977.

[83] R.J. Scheuplein, Permeability of the skin: a review of major concepts, Curr Probl Dermatol, 7 (1978) 172-186.

[84] R.E. Zimmerer, K.D. Lawson, C.J. Calvert, The effects of wearing diapers on skin, Pediatr Dermatol, 3 (1986) 95-101.

[85] J.A. Bouwstra, G.S. Gooris, J.A. van der Spek, W. Bras, Structural investigations of human stratum corneum by small-angle X-ray scattering, J Invest Dermatol, 97 (1991) 1005-1012.

[86] L.A. Barajas-Nava, J. Lopez-Alcalde, M. Roque i Figuls, I. Sola, X. Bonfill Cosp, Antibiotic prophylaxis for preventing burn wound infection, Cochrane Database Syst Rev, 6 (2013) CD008738.

[87] D. Church, S. Elsayed, O. Reid, B. Winston, R. Lindsay, Burn wound infections, Clin Microbiol Rev, 19 (2006) 403-434.

[88] M. Ansermino, C. Hemsley, Intensive care management and control of infection, BMJ, 329 (2004) 220-223.

[89] M.A. Al-Dabbagh, S. Dobson, The evidence behind prophylaxis and treatment of wound infection after surgery, Adv Exp Med Biol, 764 (2013) 141-150.

[90] M.J. Vizcaino-Alcaide, R. Herruzo-Cabrera, J. Rey-Calero, Efficacy of a broad-spectrum antibiotic (mupirocin) in an in vitro model of infected skin, Burns, 19 (1993) 392-395.

[91] A. Cadilla, M.Z. David, R.S. Daum, S. Boyle-Vavra, Association of high-level mupirocin resistance and multidrug-resistant methicillin-resistant Staphylococcus aureus at an academic center in the midwestern United States, J Clin Microbiol, 49 (2011) 95-100.

[92] J.S. Hogue, P. Buttke, L.E. Braun, M.P. Fairchok, Mupirocin resistance related to increasing mupirocin use in clinical isolates of methicillin-resistant Staphylococcus aureus in a pediatric population, J Clin Microbiol, 48 (2010) 2599-2600.

[93] J.B. Patel, R.J. Gorwitz, J.A. Jernigan, Mupirocin resistance, Clin Infect Dis, 49 (2009) 935-941.

[94] A.E. Simor, T.L. Stuart, L. Louie, C. Watt, M. Ofner-Agostini, D. Gravel, M. Mulvey, M. Loeb, A. McGeer, E. Bryce, A. Matlow, P. Canadian Nosocomial Infection Surveillance, Mupirocin-resistant, methicillin-resistant Staphylococcus aureus strains in Canadian hospitals, Antimicrob Agents Chemother, 51 (2007) 3880-3886.

[95] J.G. Hurdle, A.J. O'Neill, E. Ingham, C. Fishwick, I. Chopra, Analysis of mupirocin resistance and fitness in Staphylococcus aureus by molecular genetic and structural modeling techniques, Antimicrob Agents Chemother, 48 (2004) 4366-4376.

[96] M. Kaul, A.K. Parhi, Y. Zhang, E.J. LaVoie, S. Tuske, E. Arnold, J.E. Kerrigan, D.S. Pilch, A bactericidal guanidinomethyl biaryl that alters the dynamics of bacterial FtsZ polymerization, J Med Chem, 55 (2012) 10160-10176.

[97] G.W. Kaatz, S.M. Seo, L. O'Brien, M. Wahiduzzaman, T.J. Foster, Evidence for the existence of a multidrug efflux transporter distinct from NorA in Staphylococcus aureus, Antimicrob Agents Chemother, 44 (2000) 1404-1406.

[98] G. Sakoulas, G.M. Eliopoulos, R.C. Moellering, Jr., C. Wennersten, L. Venkataraman, R.P. Novick, H.S. Gold, Accessory gene regulator (agr) locus in geographically diverse Staphylococcus aureus isolates with reduced susceptibility to vancomycin, Antimicrob Agents Chemother, 46 (2002) 1492-1502.

[99] CLSI, Methods for Dilution Antimicrobial Sucseptibility Tests for Bacteria That Grow Aerobically; Approved Standard-Eighth Edition, Clinical and Laboratory Standards Institute, Wayne, PA, 2009.

[100] M.R. Prausnitz, R. Langer, Transdermal drug delivery, Nat Biotechnol, 26 (2008) 1261-1268.

[101] A. Arora, M.R. Prausnitz, S. Mitragotri, Micro-scale devices for transdermal drug delivery, Int J Pharm, 364 (2008) 227-236.

[102] B. Geusens, T. Strobbe, S. Bracke, P. Dynoodt, N. Sanders, M. Van Gele, J. Lambert, Lipid-mediated gene delivery to the skin, Eur J Pharm Sci, 43 (2011) 199-211.

[103] R. Notman, J. Anwar, Breaching the skin barrier--insights from molecular simulation of model membranes, Adv Drug Deliv Rev, 65 (2013) 237-250.

[104] F. Cilurzo, G. Vistoli, F. Selmin, C.G. Gennari, U.M. Musazzi, S. Franze, M. Lo Monte, P. Minghetti, An Insight into the Skin Penetration Enhancement Mechanism of N-Methylpyrrolidone, Mol Pharm, (2014).

[105] S.H. Moghadam, E. Saliaj, S.D. Wettig, C. Dong, M.V. Ivanova, J.T. Huzil, M. Foldvari, Effect of chemical permeation enhancers on stratum corneum barrier lipid organizational structure and interferon alpha permeability, Mol Pharm, 10 (2013) 2248-2260.

[106] T. Caon, L.C. Porto, A. Granada, M.P. Tagliari, M.A. Silva, C.M. Simoes, R. Borsali, V. Soldi, Chitosan-decorated polystyrene-b-poly(acrylic acid) polymersomes as novel carriers for topical delivery of finasteride, Eur J Pharm Sci, 52 (2014) 165-172.

[107] I.M. Rodriguez-Cruz, V. Merino, M. Merino, O. Diez, A. Nacher, D. Quintanar-Guerrero, Polymeric nanospheres as strategy to increase the amount of triclosan retained in the skin: passive diffusion vs. iontophoresis, J Microencapsul, 30 (2013) 72-80.

[108] A. Denis, O. Loustau, H. Chiavassa-Gandois, J. Vial, C. Lalande Champetier de Ribes, J.J. Railhac, N. Sans, [High resolution MR imaging of the skin: normal imaging features], J Radiol, 89 (2008) 873-879.

[109] A. Naik, Y.N. Kalia, R.H. Guy, Transdermal drug delivery: overcoming the skin's barrier function, Pharm Sci Technolo Today, 3 (2000) 318-326.

[110] T. Garg, G. Rath, A.K. Goyal, Comprehensive review on additives of topical dosage forms for drug delivery, Drug Deliv, (2014).

[111] S.T. Boyce, G.D. Warden, I.A. Holder, Cytotoxicity testing of topical antimicrobial agents on human keratinocytes and fibroblasts for cultured skin grafts, J Burn Care Rehabil, 16 (1995) 97-103.

[112] M.W. Casewell, R.L. Hill, Mupirocin ('pseudomonic acid')--a promising new topical antimicrobial agent, J Antimicrob Chemother, 19 (1987) 1-5.

[113] S.J. O'Day, C.J. Kim, D.S. Reintgen, Metastatic melanoma: chemotherapy to biochemotherapy, Cancer Control, 9 (2002) 31-38.

[114] A. Kim, E.H. Lee, S.H. Choi, C.K. Kim, In vitro and in vivo transfection efficiency of a novel ultradeformable cationic liposome, Biomaterials, 25 (2004) 305-313.

[115] E. McLafferty, C. Hendry, F. Alistair, The integumentary system: anatomy, physiology and function of skin, Nurs Stand, 27 (2012) 35-42.

[116] O.B. Garbuzenko, M. Saad, S. Betigeri, M. Zhang, A.A. Vetcher, V.A. Soldatenkov, D.C. Reimer, V.P. Pozharov, T. Minko, Intratracheal versus intravenous

liposomal delivery of siRNA, antisense oligonucleotides and anticancer drug, Pharm Res, 26 (2009) 382-394.

[117] S. Betigeri, M. Zhang, O. Garbuzenko, T. Minko, Non-viral systemic delivery of siRNA or antisense oligonucleotides targeted to Jun N-terminal kinase 1 prevents cellular hypoxic damage, Drug Deliv Transl Res, 1 (2011) 13-24.

[118] M. Saad, O.B. Garbuzenko, T. Minko, Co-delivery of siRNA and an anticancer drug for treatment of multidrug-resistant cancer, Nanomedicine (Lond), 3 (2008) 761-776.

[119] P. Karande, A. Jain, S. Mitragotri, Relationships between skin's electrical impedance and permeability in the presence of chemical enhancers, J Control Release, 110 (2006) 307-313.

[120] Z. Klimová, J. Hojerová, M. Lucová, S. Pažoureková, Dermal exposure to chemicals —evaluation of skin barrier damage, Acta Chimica Slovaca, 5 (2012) 70—74.

[121] S. Mourtas, S. Fotopoulou, S. Duraj, V. Sfika, C. Tsakiroglou, S.G. Antimisiaris, Liposomal drugs dispersed in hydrogels. Effect of liposome, drug and gel properties on drug release kinetics, Colloids Surf B Biointerfaces, 55 (2007) 212-221.

[122] Z. Pavelic, N. Skalko-Basnet, R. Schubert, Liposomal gels for vaginal drug delivery, Int J Pharm, 219 (2001) 139-149.

[123] T. Subongkot, B. Pamornpathomkul, T. Rojanarata, P. Opanasopit, T. Ngawhirunpat, Investigation of the mechanism of enhanced skin penetration by ultradeformable liposomes, Int J Nanomedicine, 9 (2014) 3539-3550.

[124] P. Desai, R.R. Patlolla, M. Singh, Interaction of nanoparticles and cell-penetrating peptides with skin for transdermal drug delivery, Mol Membr Biol, 27 (2010) 247-259.

[125] S. Shanmugam, C.K. Song, S. Nagayya-Sriraman, R. Baskaran, C.S. Yong, H.G. Choi, D.D. Kim, J.S. Woo, B.K. Yoo, Physicochemical characterization and skin permeation of liposome formulations containing clindamycin phosphate, Arch Pharm Res, 32 (2009) 1067-1075.

[126] J.A. McCubrey, L.S. Steelman, W.H. Chappell, S.L. Abrams, E.W. Wong, F. Chang, B. Lehmann, D.M. Terrian, M. Milella, A. Tafuri, F. Stivala, M. Libra, J. Basecke, C. Evangelisti, A.M. Martelli, R.A. Franklin, Roles of the Raf/MEK/ERK pathway in cell growth, malignant transformation and drug resistance, Biochim Biophys Acta, 1773 (2007) 1263-1284.

[127] S.R. Hingorani, M.A. Jacobetz, G.P. Robertson, M. Herlyn, D.A. Tuveson, Suppression of BRAF(V599E) in human melanoma abrogates transformation, Cancer Res, 63 (2003) 5198-5202.

[128] A. Sharma, M.A. Tran, S. Liang, A.K. Sharma, S. Amin, C.D. Smith, C. Dong, G.P. Robertson, Targeting mitogen-activated protein kinase/extracellular signal-regulated kinase kinase in the mutant (V600E) B-Raf signaling cascade effectively inhibits melanoma lung metastases, Cancer Res, 66 (2006) 8200-8209.

[129] A. Sharma, N.R. Trivedi, M.A. Zimmerman, D.A. Tuveson, C.D. Smith, G.P. Robertson, Mutant V599EB-Raf regulates growth and vascular development of malignant melanoma tumors, Cancer Res, 65 (2005) 2412-2421.

[130] M.A. Tran, C.D. Smith, M. Kester, G.P. Robertson, Combining nanoliposomal ceramide with sorafenib synergistically inhibits melanoma and breast cancer cell survival to decrease tumor development, Clin Cancer Res, 14 (2008) 3571-3581.

[131] M. Cheung, A. Sharma, S.V. Madhunapantula, G.P. Robertson, Akt3 and mutant V600E B-Raf cooperate to promote early melanoma development, Cancer Res, 68 (2008) 3429-3439.

[132] S. Tamburic, D.Q. Craig, The effects of ageing on the rheological, dielectric and mucoadhesive properties of poly(acrylic acid) gel systems, Pharm Res, 13 (1996) 279-283.

[133] A. Ortan, C.D. Parvu, M.V. Ghica, L.M. Popescu, L. Ionita, Rheological Study of a Liposomal Hydrogel Based On Carbopol, Romanian Biotechnological Letters, 16 (2011) 47-54.

[134] L. Weng, X. Chen, W. Chen, Rheological characterization of in situ crosslinkable hydrogels formulated from oxidized dextran and N-carboxyethyl chitosan, Biomacromolecules, 8 (2007) 1109-1115.

[135] A. Billard, L. Pourchet, S. Malaise, P. Alcouffe, A. Montembault, C. Ladaviere, Liposome-loaded chitosan physical hydrogel: toward a promising delayed-release biosystem, Carbohydr Polym, 115 (2015) 651-657.

[136] Z. Pavelic, N. Skalko-Basnet, R. Schubert, I. Jalsenjak, Liposomal gels for vaginal drug delivery, Methods Enzymol, 387 (2004) 287-299.